Status Report
Mu2e-II Snowmass22 Calorimeter Group

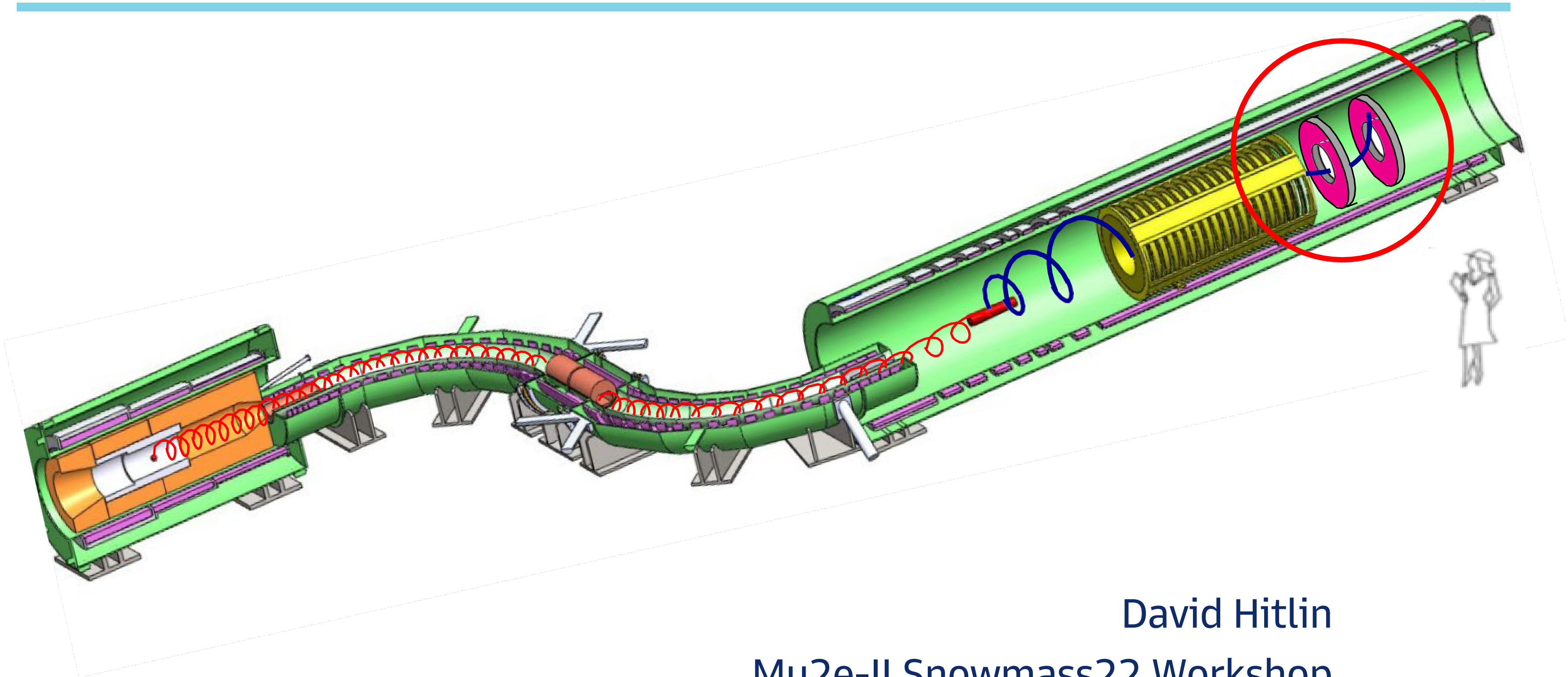

David Hitlin

Mu2e-II Snowmass22 Workshop

February 22, 2022

Frank's original charge

- "Our main item of discussion will be on issues related to whether we can handle increased beam over what has been the nominal plan. To be more explicit, I suggest:

- 1) That we take the 1.7 microsecond spill rate assumed for an aluminum stopping target
- 2) That we consider the possibility of a factor of four increase in protons in a spill, one factor of two from taking bunches at 162.5 MHz, and another factor of two from increasing the spill duration to 200 ns."

Mu2e-II Snowmass Calorimeter Group

- Convenors
  - David Hitlin, Caltech
  - Luca Morescalchi, INFN Pisa
  - Ivano Sarra, LNF

- Léo Borrell, Bertrand Echenard, Sophie Middleton, James Oyang, Frank Porter, Liyuan Zhang, Renyuan Zhu - Caltech
- Eleonora Diociaiuti, Raffaella Donghia, Simona Giovannella, Fabio Happacher, Stefano Miscetti - LNF
- Stefano Di Falco, Simone Donati, Antonio Gioiosa, Elena Pedreschi, Franco Spinella - INFN Pisa

- There has been a limited amount of activity

The nominal situation

Mu2e Calorimeter Requirements

- Mu2e-II will endeavor to maintain the performance of the Mu2e calorimeter, in a somewhat more challenging environment, re-using as much of the existing system as possible

• Energy resolution	σ < 5% (FWHM/2.36) @ 100 MeV
• Time resolution	σ < 500 ps
• Position resolution	σ < 10 mm
• Radiation hardness • Crystals • Photosensors	 1 kGy/yr and a total of 10^{12} n_1 MeV equivalent/cm^2 total 3 x 10^{11} n_1 MeV equivalent/cm^2 total
• Provide an independent standalone trigger • Provide track seeding • e/μ particle identification (reject cosmic muons by > 200) with 90% efficiency for conversion electrons • Work in a 10^{-4} Torr vacuum:	

The Mu2e-II radiation environment

- **Frank's challenge corresponds to**

- ionizing radiation (40 kGy/yr or 4 Mrad/yr)
  - Total worst case dose ~10 Mrad
- neutron levels (4 x 10^{13} n_1 MeV equivalent/cm^2 total),
-

PIP-II/Mu2e-II:

- higher rates (**~x3**) and duty factor
- correspondingly higher ionizing radiation (**10 kGy/yr**)
- neutron levels (**10^{13} $n_{\text{-1 MeV equiv}}$/cm^2 total**),

The worst case is at the inner radius of Disk 1, but radial falloff is not extreme.

Disk 2 dose is substantially lower

Nominal Mu2e-II Calorimeter Requirements

There will be higher rates, higher neutron flux and a higher ionizing dose on the photosensors

X 10 Factor →

Disk 1
Inner: (10x2x5x3) → 300 krad
Outer: (10x0.5x5x3) → 75 krad

Disk 2
Inner: (10x1x 5 x 3) → 150 krad
Outer = (10x0.5x5x3) → 75 krad

Latest SiPM Dose test indicated no hints of deterioration up to 80 krad

X 10 Factor

Disk 1 = 10 x 6 x 10^{10} x 5 x 3 = 9 x 10^{12}

Neutron fluence up to 10^{13} n_1MeV/cm^2 → -40 C

Conclusion: We need, at least in part of the calorimeter, a faster, more radiation hard scintillator, an appropriate photosensor, and a data acquisition system that can support the crystal/sensor performance

We have the needed simulation tools exist to explore the Mu2e-II parameter space
We then need an R&D program aimed at finding viable solutions

Dose per crystal in kRad/year (Mu2e)

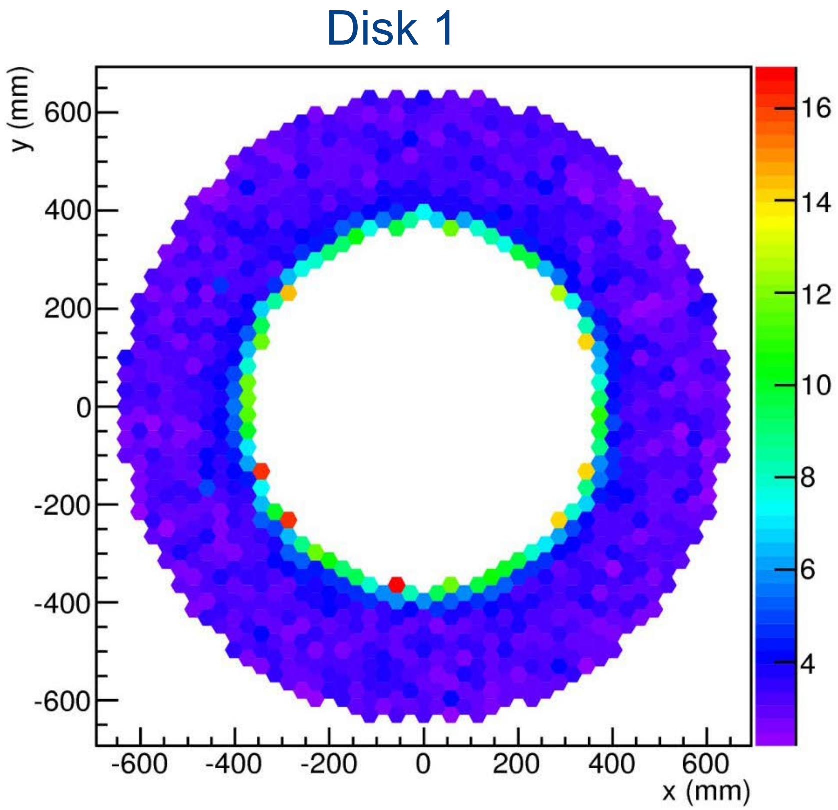

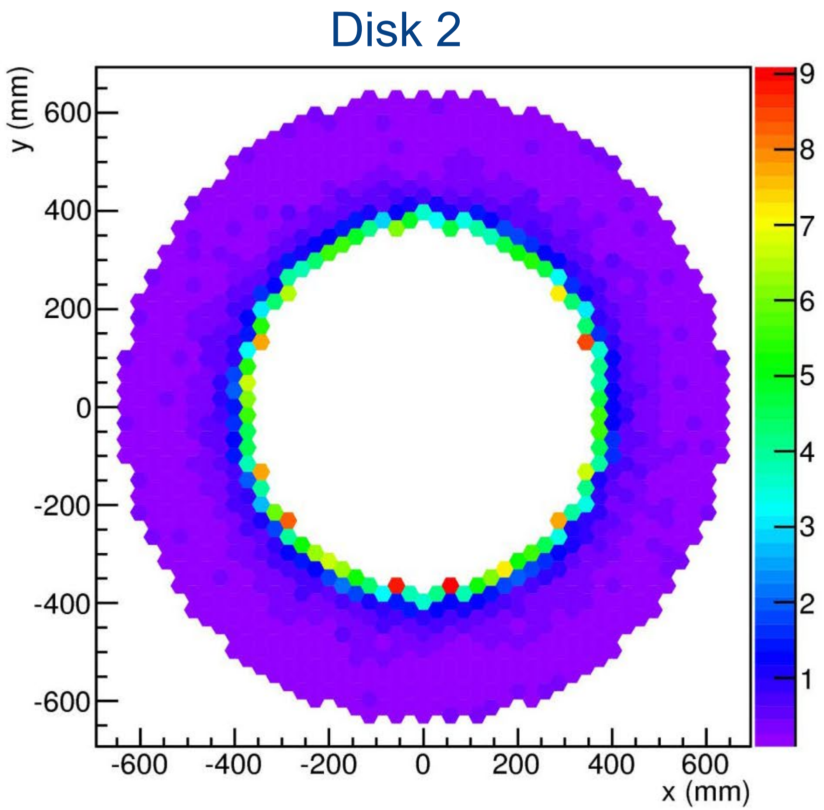

The average dose is around 3 (0.5) kRad / year for the front (back) disk, up to 16 (9) kRad / year for the innermost crystals in the front (back) disks

Echenard

Mu2e

γ Dose crystals — Neutron flux SiPMs

Disk 1

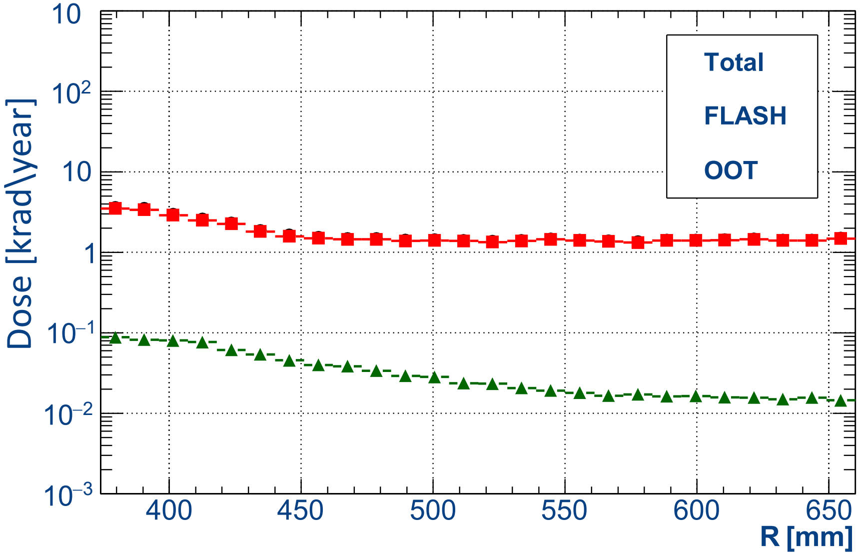

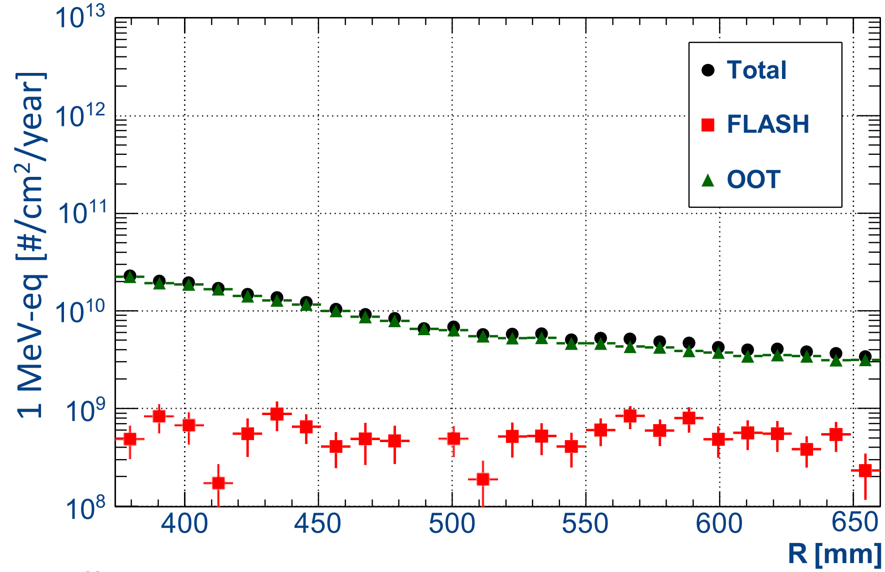

Disk 2

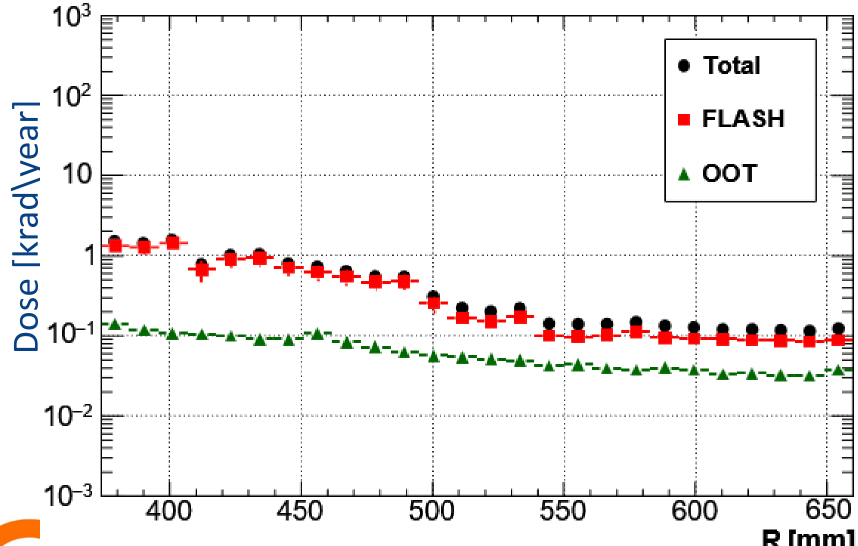

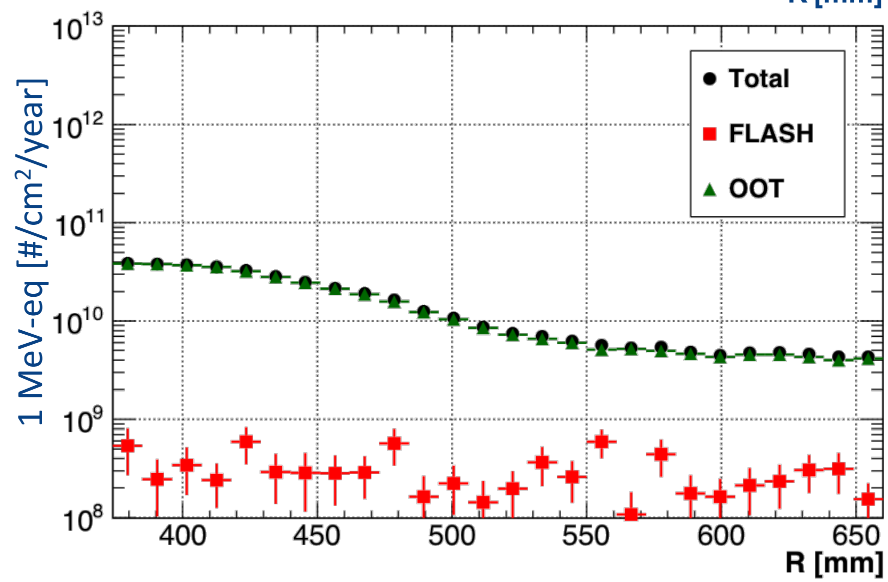

γ Dose – FEE

γ Dose – Dirac

Disk 1

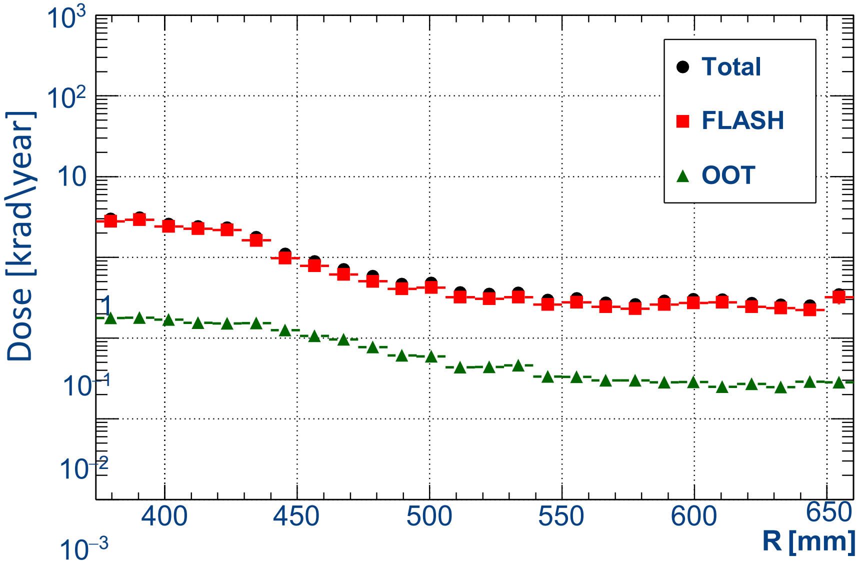

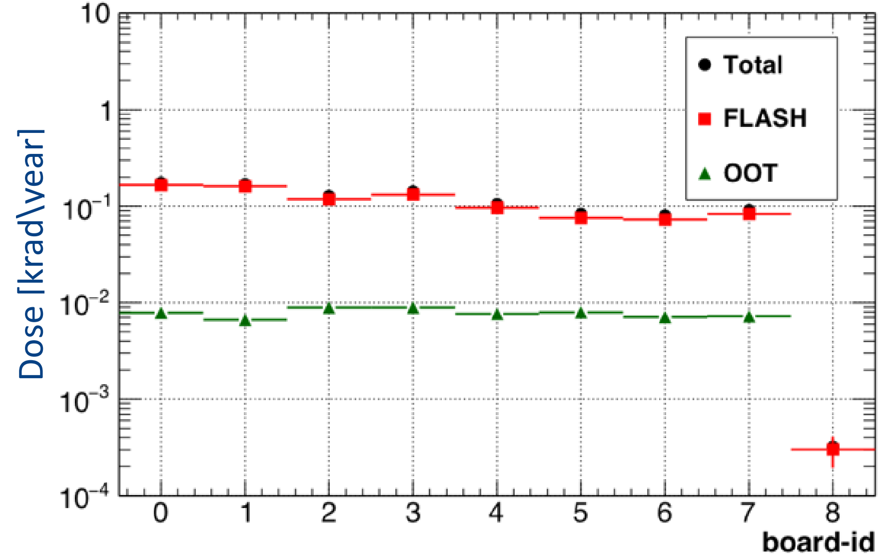

Disk 2

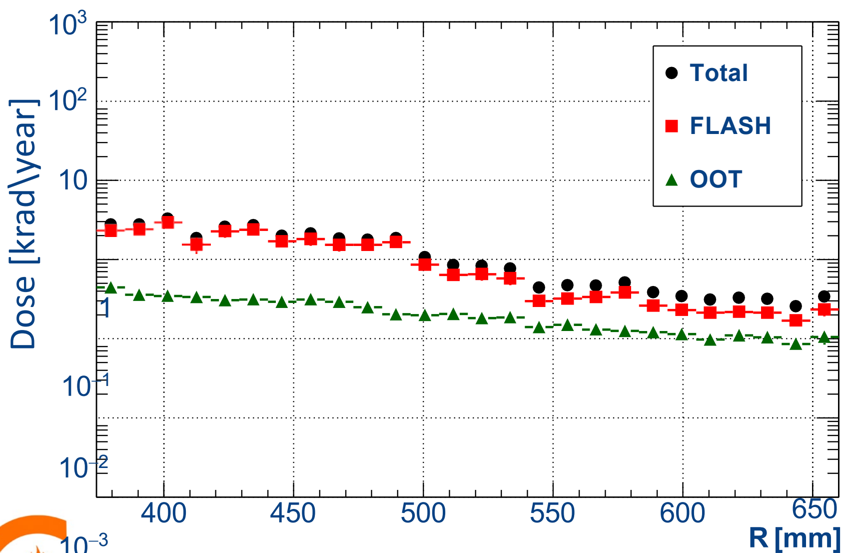

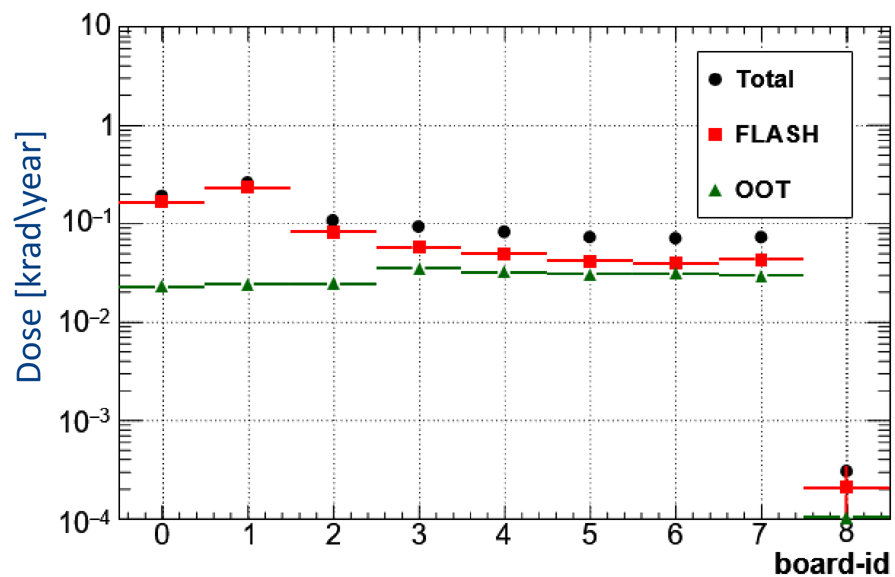

Snowmass paper section is complete

VII. CALORIMETER

A. Introduction

The calorimeter provides an alternative measurement of the conversion electron candidate's energy, as well as a fairly precise measurement of the time of energy deposit that is useful in track finding and cosmic ray rejection.

The Mu2e calorimeter design consists of pure Cesium Iodide (CsI) crystals comprising two disks. The calorimeter has robust performance at Mu2e rates but may be challenged by Mu2e-II instantaneous rates that are two to three times higher. The x10 integrated radiation dose on the calorimeter readout electronics also motivates study of appropriate rad-hard readout electronics at a level informed by the HL-LHC detector upgrades.

1. *Mu2e-II requirements*

The Mu2e-II calorimeter should have the same energy (< 10%) and time (< 500 ps) resolutions as in Mu2e, aiming to provide a standalone trigger, track seeding and PID as before. The Mu2e-II calorimeter must also withstand a higher radiation environment:

- 10^{12} - 10^{13} 1 MeV eq./cm^2 neutron flux on the photosensors and ~ 0.1 - 1 Mrad fluence on crystals;
- high rate and high pile-up probability;
- 1 Tesla magnetic field.

With respect to the dose, the second disk can perhaps be left as it is, with CsI crystals and SiPM readout, but the first disk will need a drastic change. It will be necessary to replace the CsI crystals with crystals capable of sustaining higher levels of radiation and performing at higher rates. BaF_2 crystals meet these criteria, and are a leading candidate for the Mu2e-II calorimeter.

2. *Design to meet Mu2e requirements*

An alternative calorimeter design has been developed based on barium fluoride (BaF_2) crystals readout with solar-blind UV-sensitive silicon photomultipliers that efficiently collect the very fast UV component (~220 nm) of the scintillation light while suppressing the slow component near 300 nm. This design is considerably more robust against Mu2e-II rates but requires the development and commercialization of the required solid state photosensors, which is ongoing.

B. Choice of crystal

1. *Options*

Improving on the decay time and radiation hardness of pure CsI is likely necessary to meet the more stringent requirements of Mu2e-II. LYSO:Ce is brighter, more dense and more radiation hard than CsI, but has a 40 ns decay time which is slower than CsI. LYSO:Ce is also more expensive because of the Lu_2O_3 raw material used and the higher melting point. $PbWO_4$ has a similar decay time to CsI, but a light yield of less than 10% of CsI. The radiation damage in $PbWO_4$ recovers at room temperature, requiring continuous light monitoring *in situ* to maintain calorimeter precision. Other bright and fast inorganic scintillators, such as $LaBr_3$:Ce and $CeBr_3$, are highly hygroscopic which presents a technical challenge for calorimeter construction. Table IV compares basic properties for three fast scintillating crystals which are candidates for the Mu2e-II calorimeter, where light yield is shown relative to NaI:Tl [6].

TABLE IV. Properties of three fast scintillating crystals that are practical candidates for the Mu2e-II calorimeter [6]

Crystal	X_0 cm	R_M cm	λ_I cm	$\tau_{\rm decay}$ ns	$\lambda_{\max}$ nm	Light Yield
CsI	1.86	3.57	39.3	30	310	3.6
				6		1.1
BaF_2	2.03	3.10	30.7	650	300	36
				<0.6	220	4.1
LYSO:Ce	1.14	2.07	20.9	40	402	85

Barium fluoride (BaF_2) stands out as a candidate for its ultrafast scintillation component with < 0.6 ns decay time and similar light output to CsI. Figure 19 compares the temporal response of the BaF_2 scintillation light measured by using a Hamamatsu R2059 PMT (top) and a Photek MCP-PMT 240 (bottom). While the FWHM pulse width and decay time of 3 and 1.5 ns were observed by the PMT, they are about 0.9 and 0.5 ns observed by the MCP-PMT [34]. Such an ultrafast light provides a foundation for an ultrafast BaF_2 calorimeter. A TrackToy simulation with the improved time resolution given by BaF_2 has been performed, resulting in a $\mathcal{O}(5\%)$ better sensitivity.

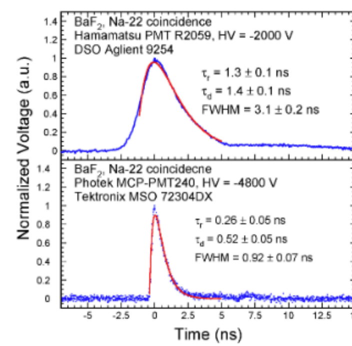

FIG. 19. A comparison of BaF_2 pulse shape measured with a Hamamatsu R2059 PMT (top) and a Photek MCP-PMT 240 (bottom).

Undoped BaF_2 also maintains its light output at high ionizing radiation levels after an initial light loss, so is more radiation hard than CsI at a large integrated dose [116]. The main issue to overcome is that its fast scintillation component at 220 nm is accompanied by a slow component at 300 nm with 650 ns decay time and a significantly larger intensity, which results in pileup and readout noise in the high-rate Mu2e-II environment.

2. *Development efforts*

Yttrium doping is found effective in suppressing the slow component while maintains the ultrafast component [32–35]. Figure 20 shows the X-ray excited emission spectra measured for BaF_2 samples with different yttrium doping level [32].

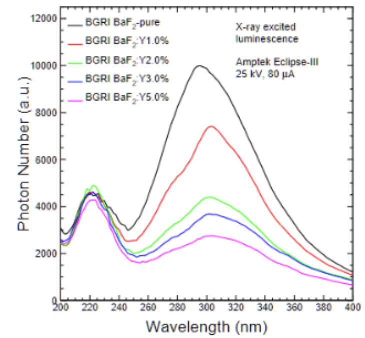

FIG. 20. X-ray excited emission spectra measured for BGRI BaF_2 crystal samples with different yttrium doping level.

R&D is on-going in collaboration with crystal producers to develop BaF_2:Y crystals of large size [37, 117]. Gamma-ray induced noise under Mu2e-II environment was measured for large size BaF_2 and BaF_2:Y crystals. Figure 21 shows photocurrent as a function of the dose rate for a BaF_2 and two BaF_2:Y samples of calorimeter size under 2 and 23 rad/h. Both yttrium doping and solar-blind photodetector are needed to reduce the gamma-ray induced readout noise to less than 0.6 MeV [117].

C. Choice of photosensor

1. *Options*

The choice of an appropriate photosensor depends, of course, on the choice of scintillator.

There are already large area SiPMs appropriate for the readout of pure CsI and for LYSO:Ce. The only major concern is radiation hardness in the Mu2e-II environment, particularly for low energy neutrons.

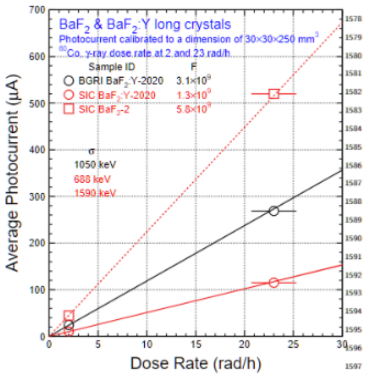

FIG. 21. Photocurrent is shown as a function of the dose rate for an SIC BaF_2 and two BGRI and SIC BaF_2:Y samples of calorimeter size under ionization dose rate of 2 and 23 rad/h.

An appropriate large area photosensor for BaF_2 for use in the Mu2e-II calorimeter must meet additional several criteria: It must have good quantum efficiency for the 220 nm fast component while being insensitive to the 300 nm slow component, must be radiation hard, must work in an axial magnetic field and must have as fast a time response as possible.

There are several candidates for such a sensor. All require additional R&D efforts before a fully appropriate photosensor can be identified. These are discussed below.

2. *Development efforts*

There are several potential approaches. A microchannel plate photomultiplier is very fast and works in a magnetic field. It can be equipped with a photocathode such AlGaN, which is UV-sensitive and solar-blind, and thus a good match to the BaF_2 fast component, with quantum efficiency as high as 30%. Such devices have been used in astrophysics for years. The problem is that even with recent advances in MCP longevity due to the application of ALD coatings to the MCP (to lifetimes of tens of coulombs/cm^2), they cannot cope by many orders of magnitude, with the integrated radiation dose of Mu2e-II.

LAPPDs with UV-extended photocathodes such as Cs_2Te are an attractive, and possibly less expensive, alternative. They could perhaps be developed on the needed time scale, but again the question of longevity of the MCP in the Mu2e-II environment is an issue.

Wavelength-shifting techniques, particularly involving nanoparticles, are being explored. Specific formulations have been applied to MPPCs operating in photovoltaic mode.

Atomic-layer-deposition (ALD) bandpass filters integrated with the silicon structure of the photosensor promise several advantages. These can be either avalanche photodiode [118] or silicon photomultiplier devices [119]; work has been done on both. These have excellent quantum efficiency at 220 nm, strong rejection of 300 nm response, time response superior to existing SiPMs and adequate longevity in the face of exposure to strong UV radiation. The ultimate realization of this concept would be a back-illuminated device with delta doping to improve the time response and resistance to degradation from the incident UV radiation. Figure 22 shows scintillation spectrum of pure BaF_2 and BaF_2 doped with 6% Y, compared with the measured PDE of a 6 × 6mm SiPM with an integrated filter [35].

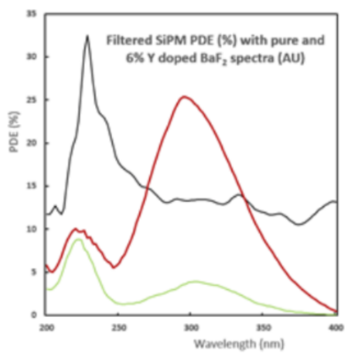

FIG. 22. Scintillation spectrum of pure BaF_2 and BaF_2 doped with 6% Y, compared with the measured PDE of a 6 × 6mm SiPM with an integrated filter.

D. Data acquisition options

The Mu2e electromagnetic calorimeter DAQ uses custom waveform digitizers mounted inside the magnet cryostat. The system is qualified for a TID of up to 20 krad, and samples SiPM signals at 200 MHz. Serial data readout is through a 4.8 Gbit link. The expected Mu2e-II instantaneous event rate will be about three times higher than in Mu2e and will generate a ten times larger data sample; the integrated radiation dose absorbed by the electronics will be ten times higher as well. Given the expected high rates, the shaping time will have to be reduced and therefore the 200 MHz digitizers employed in Mu2e will be inadequate. In the next few years, an intense R&D campaign will be carried out to evaluate possible alternatives, which will be driven mostly by the choice of crystal and photodetector. These alternatives include:

- A faster waveform digitizer system. Sampling at 1 GHz will be sufficient to solve pile-up and measure the pulse time and energy. Due to the much higher data flow, raw data will need to be processed inside the digitizer board; only physics related parameters (energy, time, quality, ...) will be transmitted to the central DAQ, a choice that will reduce the needed bandwidth. Several challenges remain, including availability of rad hard fast ADCs and high performance FPGAs, cost and power dissipation.

- A pure TDC system. CERN has developed a new 64-channel ps resolution TDC, rad-hard, named the Pico TDC. In principle, this would solve the bandwidth problem. The required FPGA performance would be limited and would allow the use of commercial low-cost rad hard components, such as a Xilinx Kintex or a Microsemi Polarfire. Unfortunately, TDCs do not solve the pile-up problem and energy resolution is quite low. A detailed Monte Carlo simulation will be needed to explore this option.

- A multi-level TDC system. Given the limited number of calorimeter channels, it is possible to transmit the data of one channel to several discriminators with increasing thresholds. A system with between 4 and 8 thresholds would be possible with less than 200 Pico TDCs. The conversion of the same pulse time at different heights would help resolve the pile-up problem, and also improve the energy resolution. Data could be interpolated on the fly with a limited performance rad hard FPGA.

- A mixed system with a TDC plus a relatively slow ADC system. This solution would help to solve the pile-up while retaining optimal time resolution. The ADC speed could be limited to 40 MHz, to be confirmed by Monte Carlo simulations. TDC and ADC data could be combined on the fly by the onboard FPGA which would return only the pulse parameters, thus limiting the employed bandwidth.

E. Stopping target monitor

In order to measure the denominator of $R_{\mu e}$ the number of captured muons must be determined. In Mu2e this is done by the Stopping Target Monitor (STM) which monitors X- and γ - rays emitted at the stopping target during the muon capture process. The detector looks for characteristic emission lines, for an aluminum target:

1. a 347 keV emission from the $2p \to 1s$ transition, which is prompt with the muon stop,

2. a 1809 keV emission from the nuclear capture, with the characteristic muonic aluminum lifetime of 864 ns, and

3. a 844 keV emission from the decay of the meta-stable ^{26}Mg* capture product, with a lifetime of 9.5 min.

In Mu2e the STM consists of a pair of detectors: a high-purity germanium (HPGe) solid-state photon detector, operated at liquid nitrogen temperatures, and a scintillating crystal $LaBr_3$ calorimeter. These detectors complement one-another. The HPGe has an excellent resolution of 1-2 keV and the $LaBr_3$ is capable of handling high rates and has excellent radiation hardness. These detectors are housed in a shielded enclosure, and view the muon stopping target through a collimation system and vacuum window from a distance of about 34 m. The large distance, small collimator openings, and plastic absorber placed between the stopping target and detectors should reduce the photon rate to manageable levels. These two detectors aim to measure the capture rate to an accuracy of 10%.

The Mu2e-II environment poses significant challenges for the HPGe detector:

- HPGe has a slow recovery time. The passage of the beam through the stopping target foils leads to an extremely intense bremsstrahlung flash ("beam flash"), with a high end-point energy of order 60MeV - an order of magnitude larger than our highest signal energy. The system of collimators developed for Mu2e may be not be able to handle the higher rates of Mu2e-II.

- The resolution of the HPGe detector will suffer from neutron-induced displacement damage.

There are a number of ways to mitigate against the above issues and continue to use the HPGe and $LaBr_3$ in Mu2e-II:

1. Reduce the "beam flash" by increasing the absorber thickness in the STM beamline, this will, however, result in loss of signal rate;

2. Utilize the high resolution of the HPGe to identify and separate contaminant peaks in the neighborhood of signal lines during special low intensity runs, and use that data to calibrate the $LaBr_3$ detector;

3. The flash is highly directional, while the signal lines are isotropic, moving the detectors off-axis could help, however, there is limited space in the experimental hall, so this may not be feasible;

4. Replace some crystals in the calorimeter with LYSO or $LaBr_3$, this makes absolute calibration difficult;

5. Create a tertiary photon beam and view that instead. Compton scattering and Bragg diffraction offer two alternatives.

To summarize, the STM provides an in-situ measurement of the muon capture rate at the stopping target, at an accuracy of 10%. In order use the same technology as is used in Mu2e in Mu2e-II significant revisions are required. The more intense environment at Mu2e-II provides higher rates and larger potential neutron damage which can prevent the STM detectors achieving the required resolution. Several potentially extensive modifications are outlined which might help mitigate these issues, however, R&D is required to understand the capabilities for the future. Additional ideas, including completely new concepts for monitoring schemes, are welcome and encouraged.

TABLE IV. Properties of three fast scintillating crystals that are practical candidates for the Mu2e-II calorimeter [6]

Crystal	X_0 cm	R_M cm	λ_I cm	τ_{decay} ns	λ_{max} nm	Light Yield
CsI	1.86	3.57	39.3	30	310	3.6
				6		1.1
BaF_2	2.03	3.10	30.7	650	300	36
				<0.6	220	4.1
LYSO:Ce	1.14	2.07	20.9	40	402	85

Fast Inorganic Scintillators

	GSO	YSO	LSO/ LYSO	CsI	BaF_2	CeF_3	$CeBr_3$	$LaCl_3$	$LaBr_3$
Density (g/cm^3)	6.71	4.44	7.4	4.51	4.89	6.16	5.23	3.86	5.29
Melting point (℃)	1950	1980	2050	621	1280	1460	722	858	783
Radiation Length (cm)	1.38	3.11	1.14	1.86	2.03	1.7	1.96	2.81	1.88
Molière Radius (cm)	2.23	2.93	2.07	3.57	3.1	2.41	2.97	3.71	2.85
Interaction Length (cm)	22.2	27.9	20.9	39.3	30.7	23.2	31.5	37.6	30.4
Weighted Z value	57.9	33.3	64.8	54	51.6	50.8	45.6	47.3	45.6
dE/dx (MeV/cm)	8.88	6.56	9.55	5.56	6.52	8.42	6.65	5.27	6.9
Peak Emission [a] (nm)	430	420	420	420 310	300 220	340 300	371	335	356
Refractive Index[b]	1.85	1.8	1.82	1.95	1.5	1.62	1.9	1.9	1.9
Relative Light Yield[a]	45	76	100	4.2 1.3	42 4.8	8.6	99	15 49	153
Decay Time[a] (ns)	73	60	40	30 6	650 0.6	30	17	570 24	20
d(LY)/dT [d] (%/°C)	-0.4	-0.1	-0.2	-1.4	-1.9 0.1	~0	-0.1	0.1	0.2

a. Top line: slow component, bottom line: fast component.
b. At the wavelength of the emission maximum.
c. Relative light yield normalized to the light yield of LSO
d. At room temperature (20°C) #. Softening point

1. http://www.detectors.saint-gobain.com/Plastic-Scintillator.aspx

http://pdg.lbl.gov/2008/AtomicNuclearProperties/HTML_PAGES/216.html

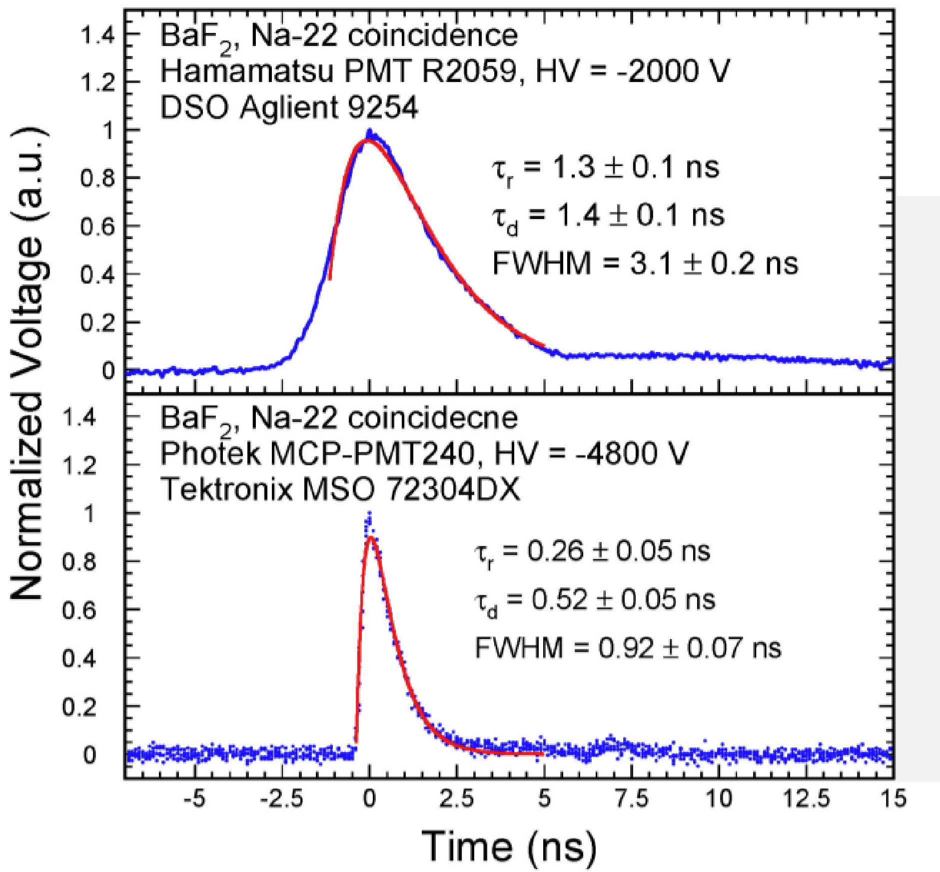

FIG. 19. A comparison of BaF_2 pulse shape measured with a Hamamatsu R2059 PMT (top) and a Photek MCP-PMT 240 (bottom).

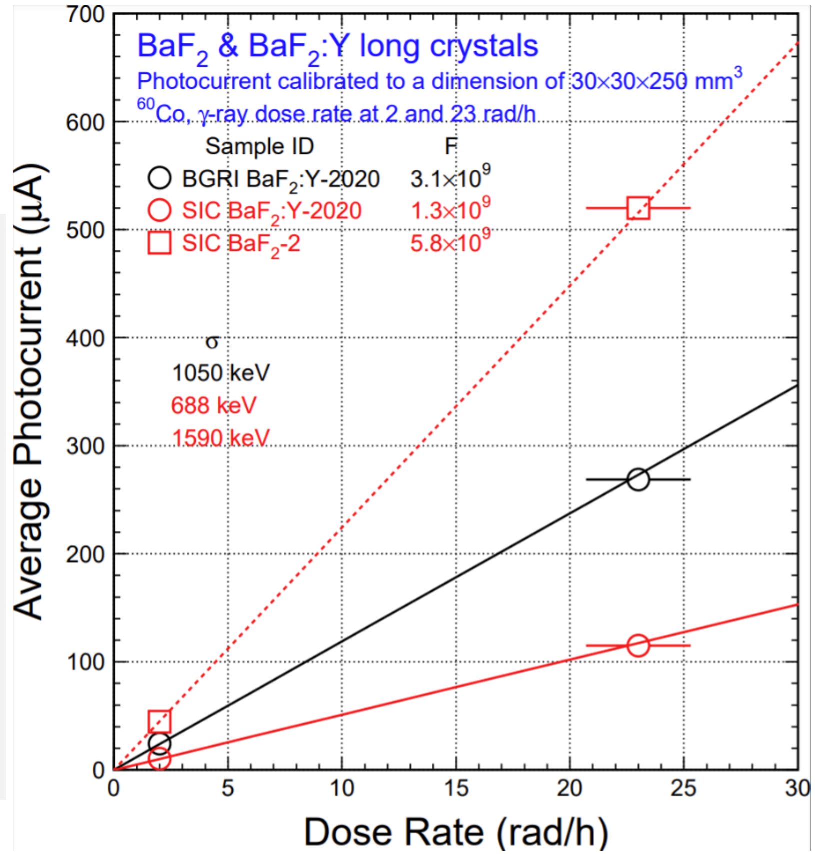

FIG. 21. Photocurrent is shown as a function of the dose rate for an SIC BaF_2 and two BGRI and SIC BaF_2:Y samples of calorimeter size under ionization dose rate of 2 and 23 rad/h.

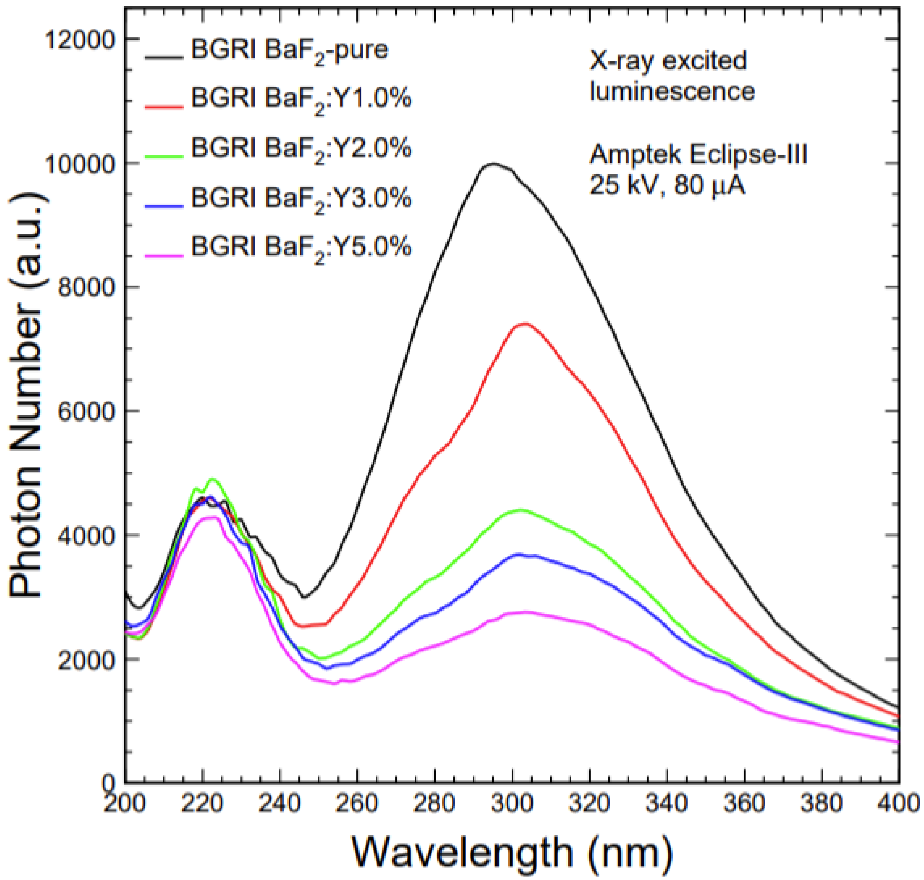

FIG. 20. X-ray excited emission spectra measured for BGRI BaF_2 crystal samples with different yttrium doping level.

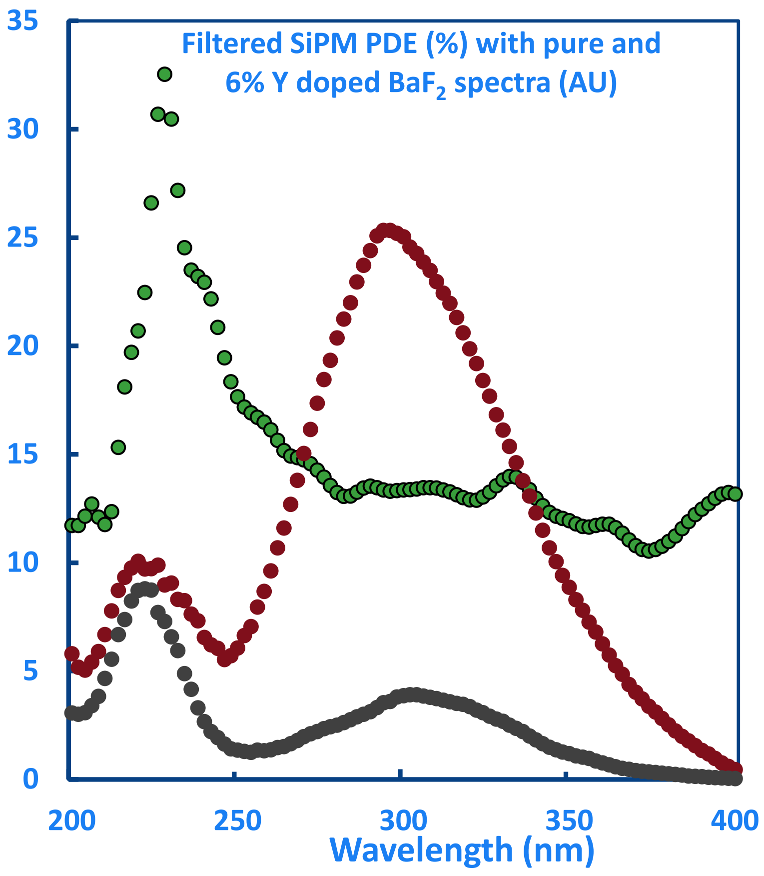

FIG. 22. Scintillation spectrum of pure BaF_2 and BaF_2 doped with 6% Y, compared with the measured PDE of a 6 × 6mm SiPM with an integrated filter.

New result – not in paper

- PDE of five-layer filter
- The good news
  - Better centering on fast component
  - Better suppression of slow component
- The bad news
  - Higher leakage current $\Rightarrow$ more noise
  - Lower PDE at peak
- Next step is to run at lower temperature to characterize leakage current and PDE
  - ready to go

- We have no funding to pursue the delta-doped, back illuminated version needed for Mu2e-II, so this appears to be the end of the story for the present

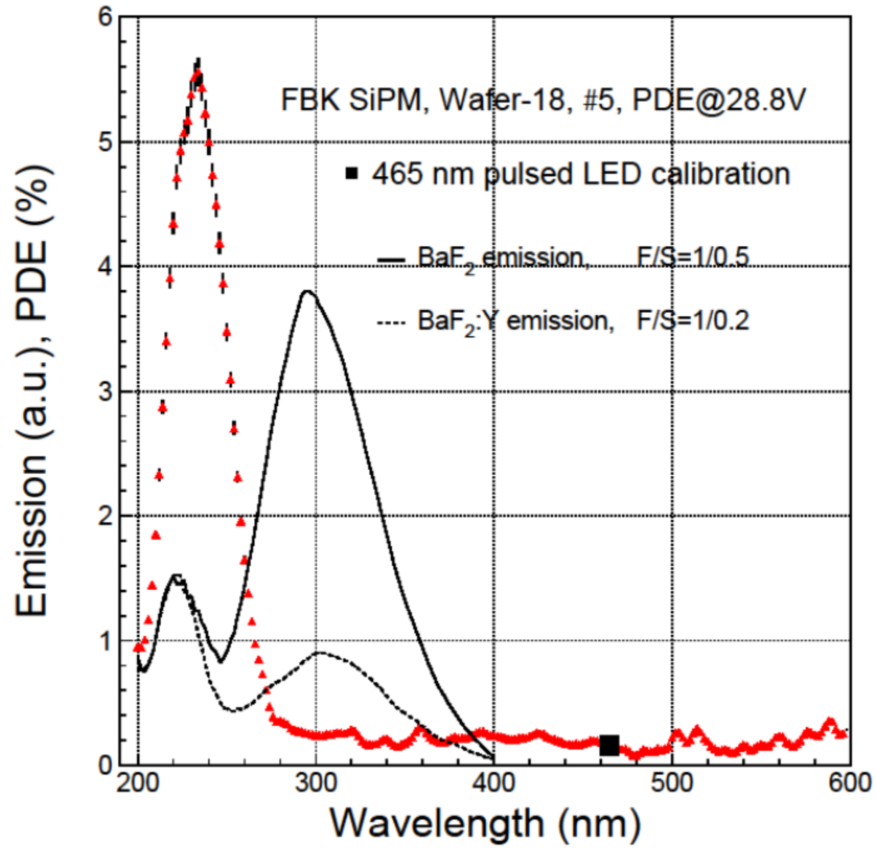

Radiation hardness comparison

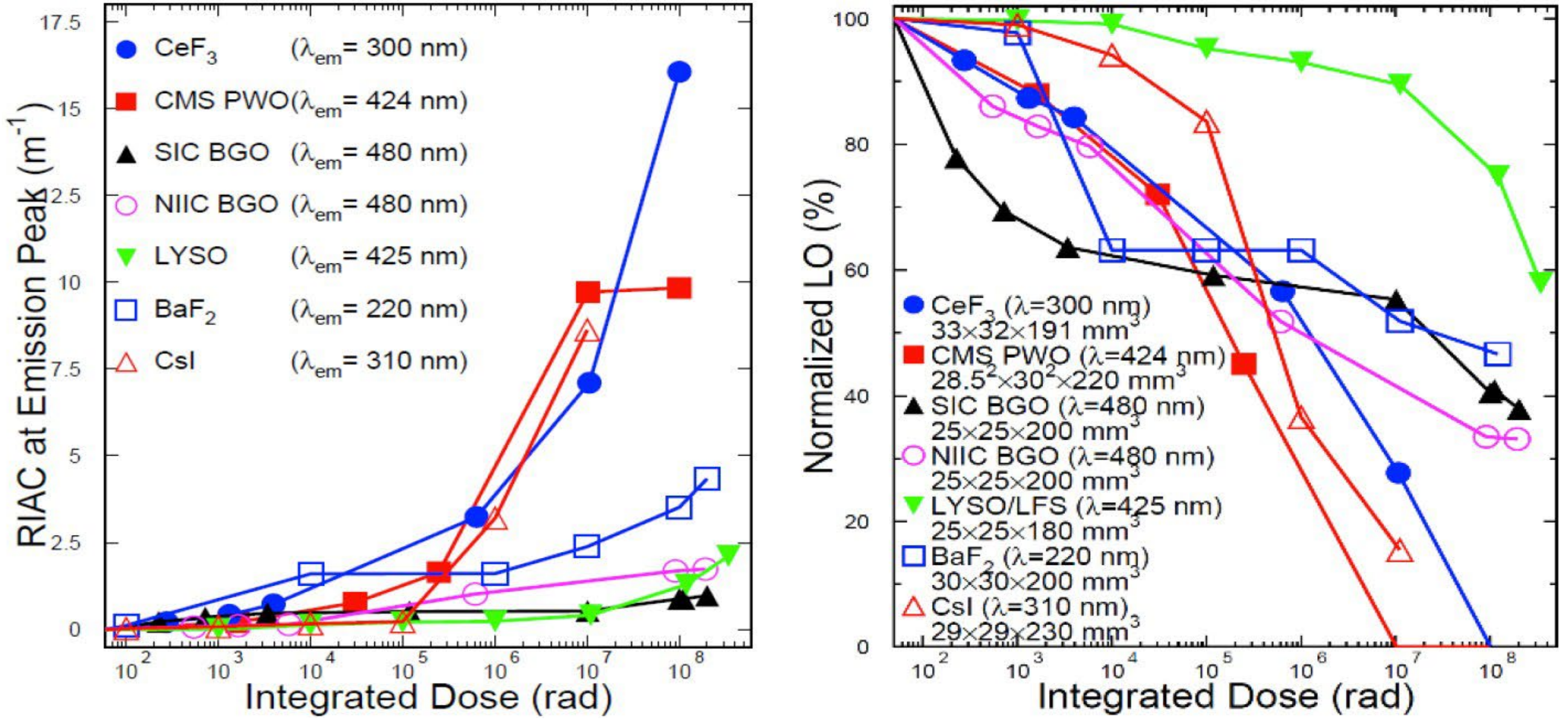

R.Y. Zhu

RIAC: radiation induced absorption coefficient

For radiation hardness, the leading candidates are BaF_2 and LYSO

Radiation hardness of Y-doped BaF_2

- Caltech plans to study the light output change of BaF_2(Y) under γ irradiation
  Dubna has done tests with reactor neutrons up to ~2.3×10^{14} n/cm^2 with BaF_2(Y) samples from SICCAS and BGRI
- In unirradiated samples, the slow signal is suppressed 3.6 times in the 1at.% doped sample, 7.2 times in the 3at.% doped sample and ~7.5 times in the 5at.% doped sample compared to the slow component of a pure BaF_2 sample

Fast emission LO, ph.e.

Y doping	0%	1at.%	3at.%	5at.%
Unirradiated	**57.4**	57.2	55.9	52.7
Irradiated	53.0	48.0	46.5	44.1
LO_{Irr}/LO_{Unirr}	0.923	0.84	0.83	0.84

Slow emission LO, ph.e.

Y doping	0%	1at.%	3at.%	5at.%
Unirradiated	**526**	146	71	67
Irradiated	490	125	60	58
LO_{Irr}/LO_{Unirr}	0.93	0.856	0.845	0.866

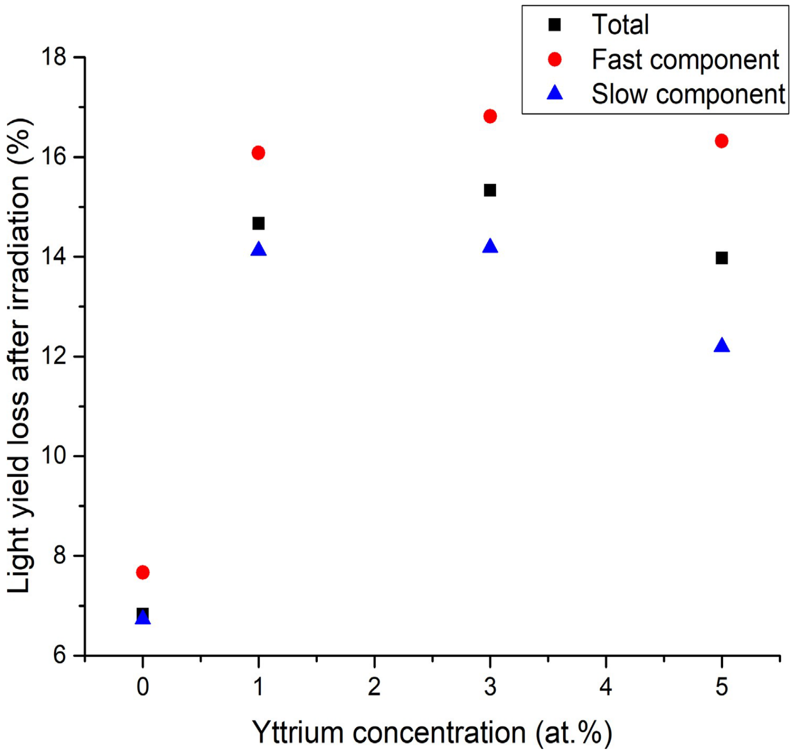

Y. Davydov

Photosensor

- The likely viable photosensor will be some type of SiPM
  - Conventional (UV-extended) SiPMs are compatible with LYSO and CsI
  - We have a first generation filtered UV-extended SiPM for BaF_2

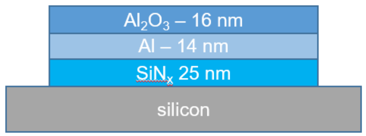

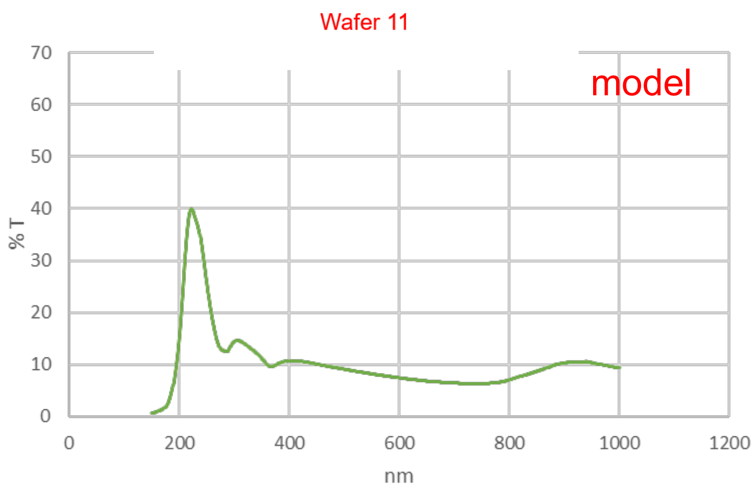

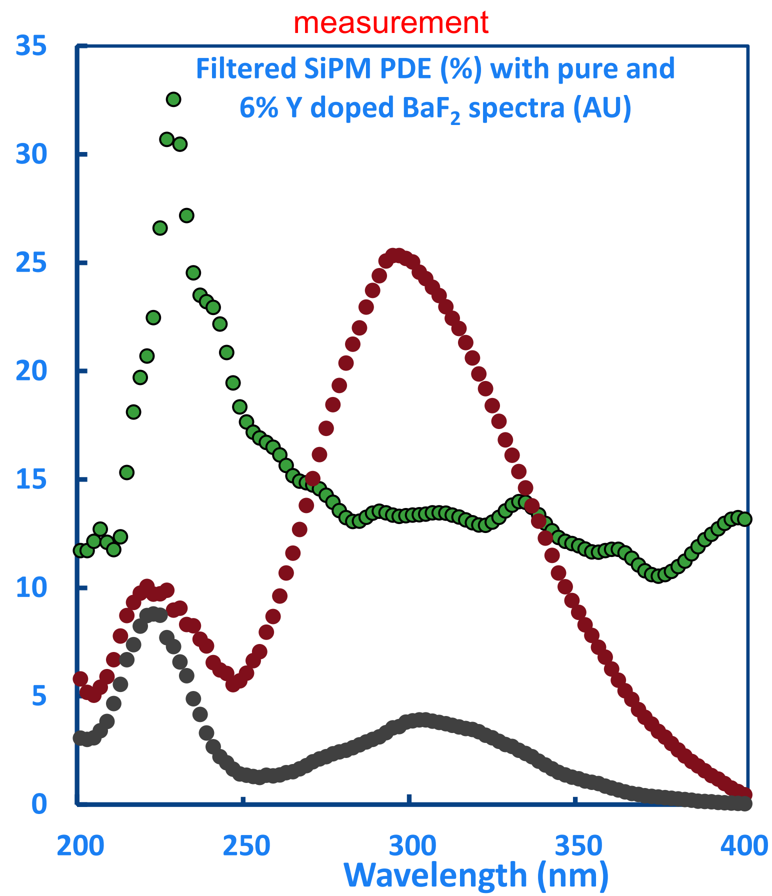

- Neutron dose is the largest concern
  - Reduced temperature operation is the response
- Pulse shaping will be required

Hamamatsu VUV MPPC

<u>S13370 series</u>

- High PDE in VUV wavelength range
  - No slow/fast component discrimination
- Low optical crosstalk through trench structure
- Typical decay time of a large area device, dictated by RC
- 4@ 6x6mm
- Work at cryogenic temperatures

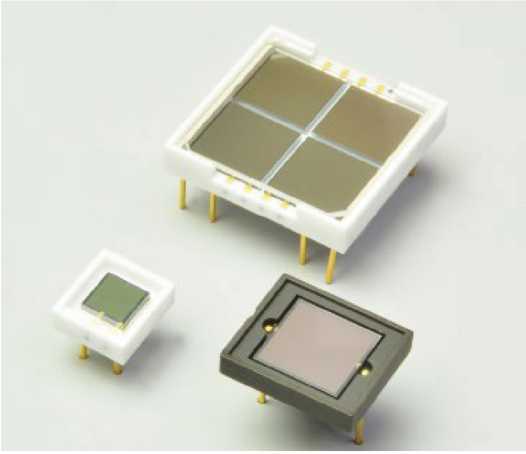

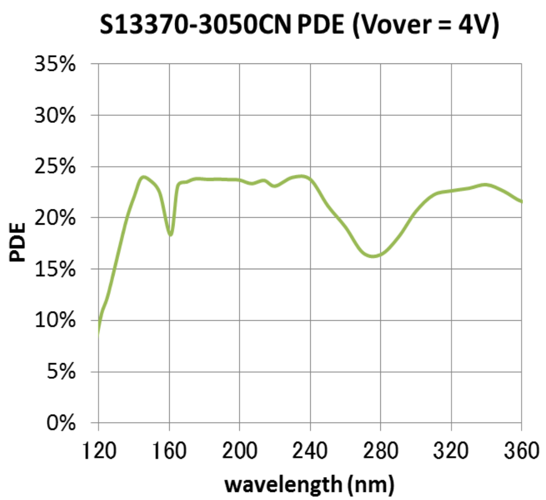

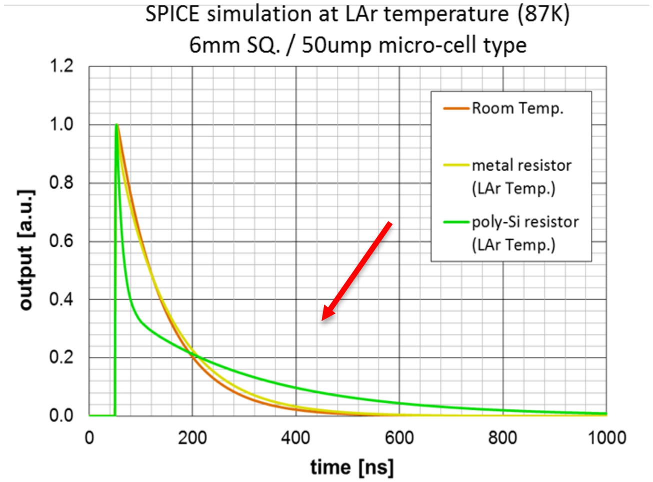

Series/parallel connection of 6x6 mm SiPMs, as in the current Mu2e calorimeter, improves decay time characteristics

- FBK also has excellent VUV SiPMs

Photosensor options for Y-doped BaF_2

- We still lack an ideal photosensor for the rates of Mu2e-II
- What is required of an appropriate photosensor?
  - Spectral sensitivity in the 200 nm region for best energy and time resolution
  - Fast/slow component discrimination for high rate capability
  - Improved rise/fall time characteristics to fully capitalize on the fast component native time resolution and rate capability
  - Radiation hardness (photons/neutrons)
  - Must work in a 1T magnetic field
- Photosensor candidates
  - External filters or nanoparticle wavelength shifters
  - Integrated filters
    - Large area APD, having 50% PDE at 220nm and strong suppression at 320nm developed at Caltech/JPL/RMD
      - These have larger dark current and more noise than standard RMD devices, but could be run at reduced temperatures
    - Large area SiPMs with an integrated filter and potentially improved time response are currently under development at Caltech/JPL/FBK
  - MCPs
    - LAPPDs such as those from Incom, with solar blind photocathodes
    - AlGaN photocathodes + MCP (Dubna)

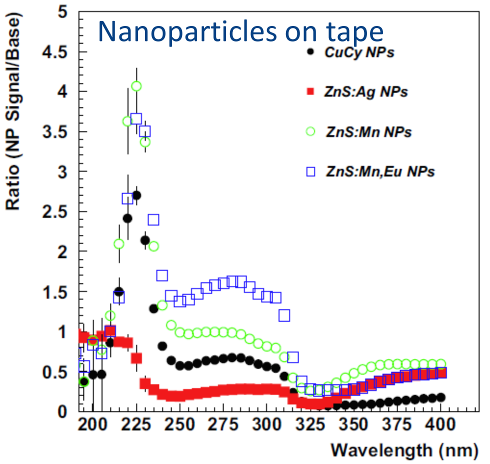

PMT + external filter

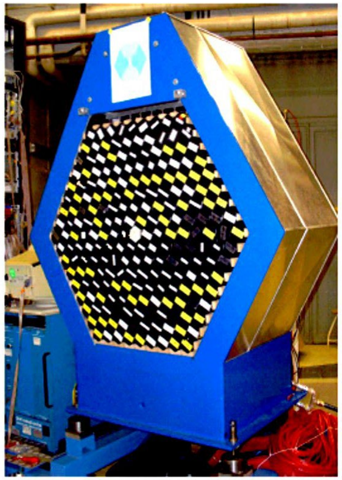

- The TAPS experiment at ELSA at Mainz (no B field) has for many years had a BaF_2 forward calorimeter, reading out both fast and slow components with HR2059-01 PMTs
  - They use an integration time of 2μs; they are thus limited to a single crystal rate of ~100kHz
- An upgrade must cope with increased rates, so they eliminate the slow component using a bandpass filter centered at 214 nm with a transmission at λ_{max} that varies from 36 to 42%
- Elimination of the slow component allows a gate of 20ns, with a resulting single crystal rate capability up to ~2 MHz

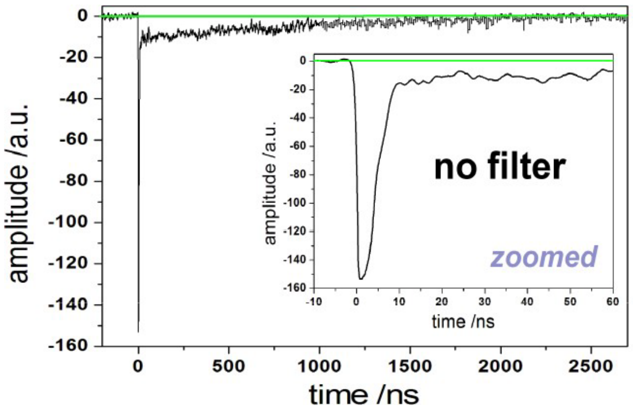

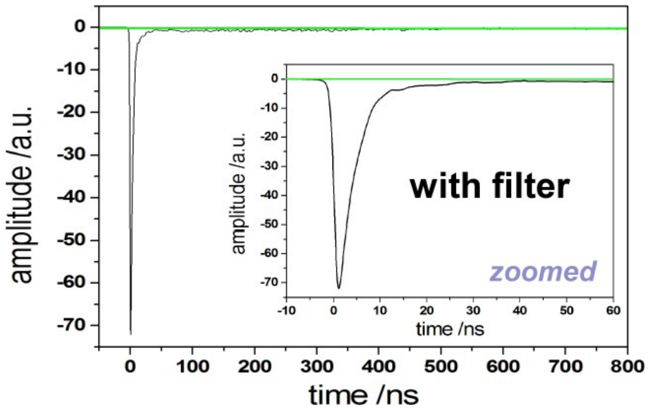

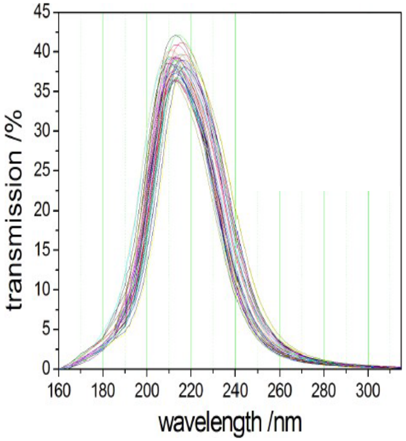

S. Diehl, R.W. Novotny, B. Wohlfahrt and R. Beck, CALOR 2014

An external filter can also be used with an appropriate solid state photosensor However, an filter integrated with the silicon sensor can achieve greater efficiency

Integrated approaches

- The LAPPD, a channel plate PMT that works in a magnetic field, is very fast and potentially very attractive, but a great deal of R&D remains before we have practical device for use with BaF_2
  - Need either a photocathode with an extended UV response and a quartz entrance window (*i.e.*, no filter), or
  - An efficient filter and/or wavelength-shifting coating on the window
  - A size appropriate to the scintillating crystal Molière radius
  - An affordable price

  - DH and RYZ had initiated an effort with ANL to develop an 8x8 cm LAAPD with a Cs_2Te UV-extended solar-blind photocathode
    - After preliminary discussions, this effort has been suspended

AlGaN photocathodes for an MCP

- AlGaN photocathodes have UV sensitivity and are solar-blind
- Have been used in astrophysics for years, QE_{opaque} ~30% at 220 nm
- Wide-band semiconductors such as AlGaN are radiation-hard

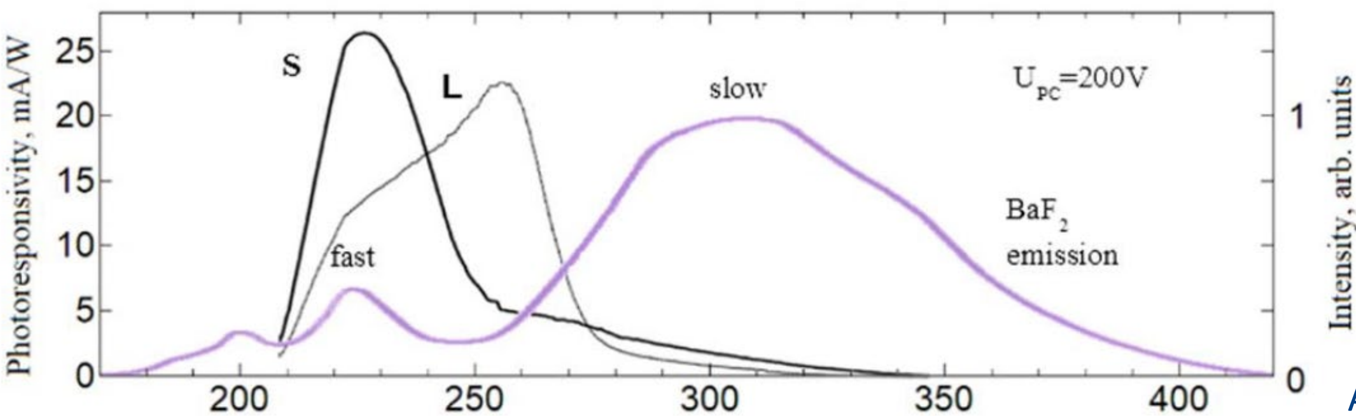

Atanov, et al.

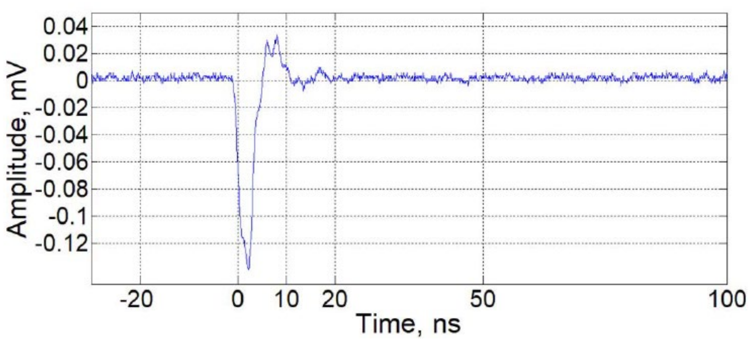

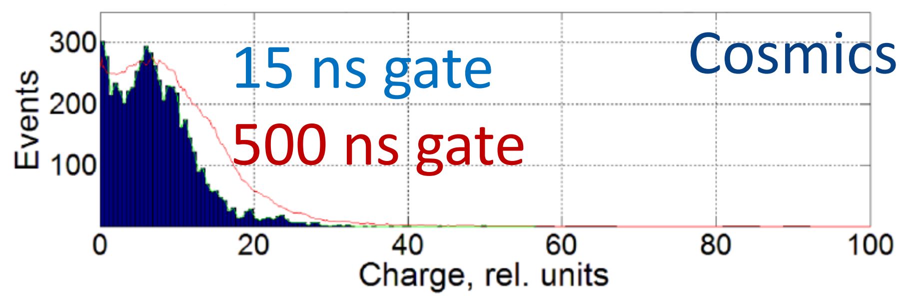

What is the lifetime in total charge at the anode of the MCP?

LAPPD with solar blind photocathode

- The LAPPD, a channel plate PMT now produced by Incom in 20x20cm size, is very fast and potentially very attractive, but much R&D remains before we have a practical device for use with BaF_2
  - Quartz entrance window
  - Cs-Te or AlGaN photocathode
  - A size appropriate to the scintillating crystal Molière radius
  - An affordable price

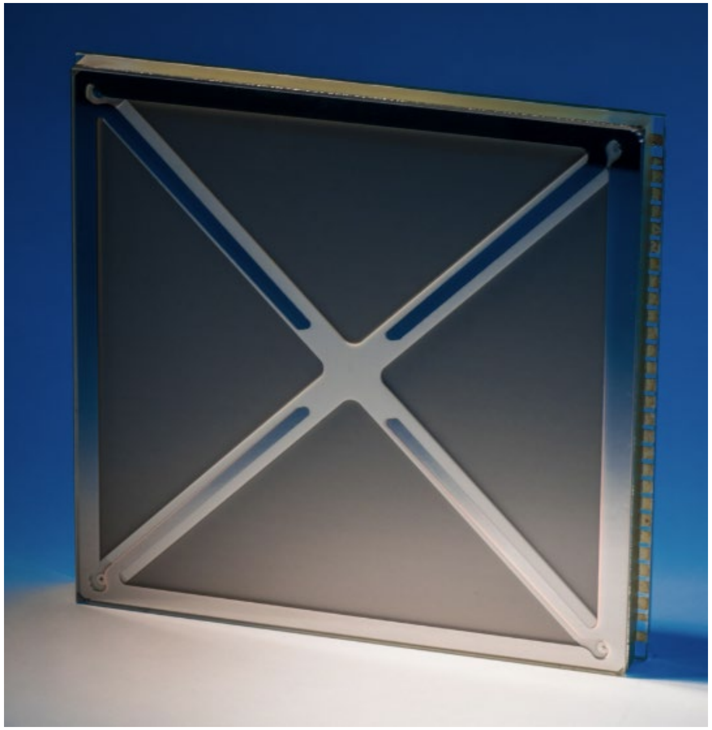

An abortive attempt to develop such a device using existing equipment was launched by ANL/Caltech, but was killed when ANL HEP Division management changed

What is the lifetime in total charge at the anode of the MCP?

Mu2e

- Mu2e-II beam luminosity is 3x; we will have 3 times more hits …
  - We have to change detector strategy … (pile-up explosion …)
- Let's assume the same architecture: crystal + photodetector, and almost the same specs: timing resolution $\mathcal{O}$ 200 ps, energy resolution $\mathcal{O}$ 10 %
  - We need faster crystal (BaF_2, …) and faster analog electronics (shaping amplifier)
- Assume shaped signal width $\mathcal{O}$ 30 ns with a rise time $\mathcal{O}$ 5 ns

- Mu2e readout is based on 200 MHz 12 bit ADCs, shaper is tuned for rise time $\mathcal{O}$ 25 – 30 ns so we can have 5-6 samples to calculate t_0.
- We need a different readout scheme to reach the same requested $\mathcal{O}$ 200 ps timing resolution

Mu2e event

- Current Mu2e ecal event (simulation, 1 channel, inner ring, crowded ...)

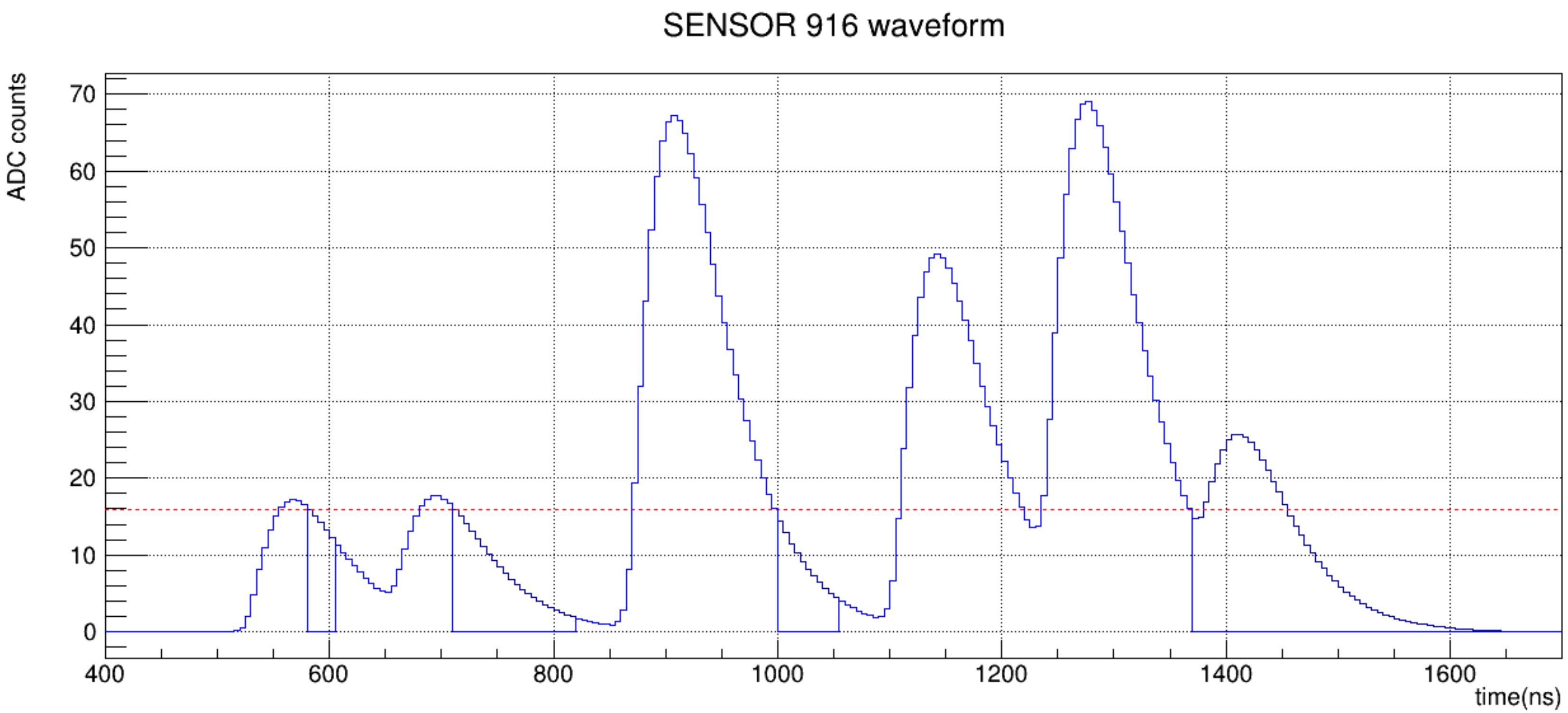

- One hit 100-200 ns
-

Mu2e event ⇨ Mu2e-II event

- Current Mu2e ecal event (simulation, 1 channel, inner ring, crowded …)

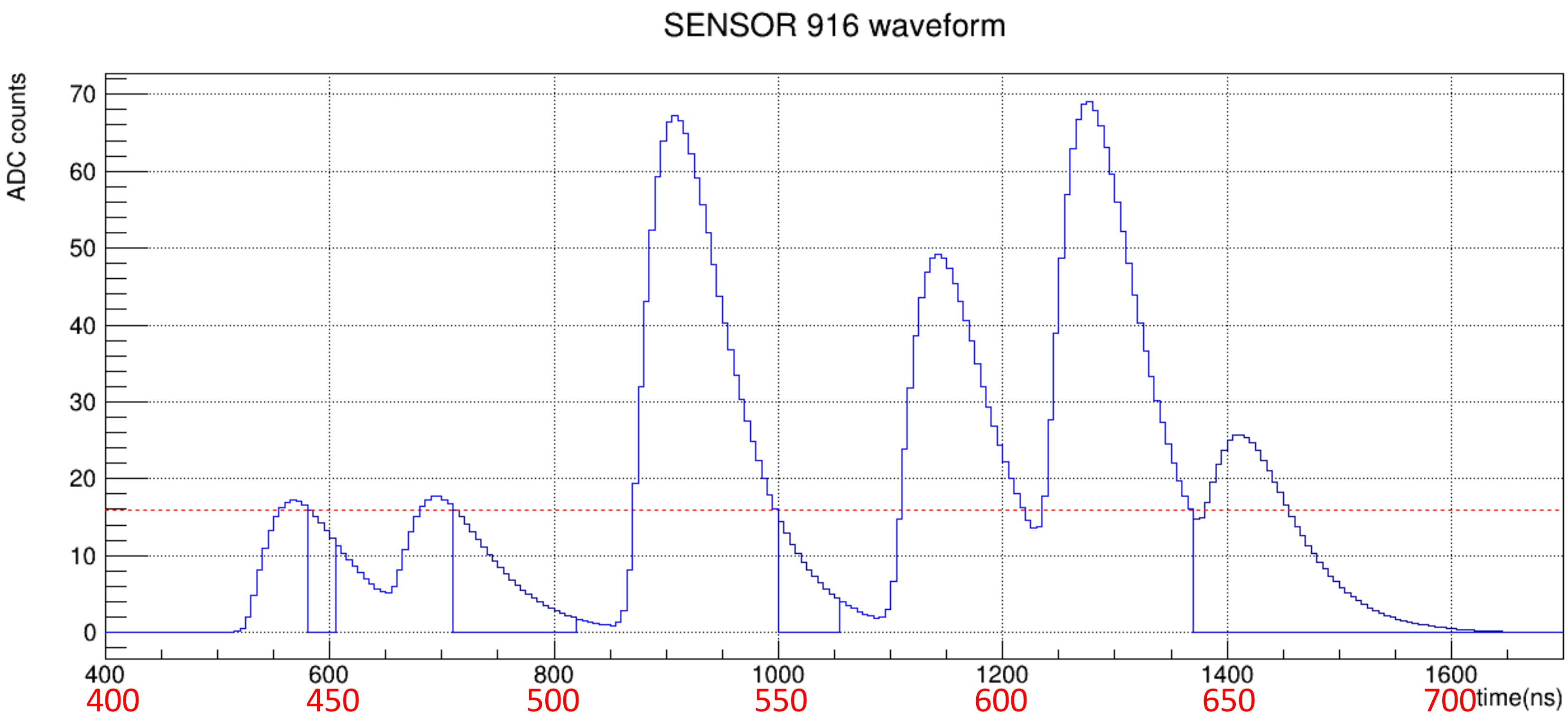

- One hit 100- 200 ns
- One hit 30- 50 ns

Luca's comments on DAQ

- At the moment it isn't possible to say what the maximum rate capability we will be able to sustain in Mu2e-II from the point of view of the electronics.
  - This will depend on the technology that will be available at the moment
  - the main concern, as Franco Spinella showed in his workshop talk, will be the **radiation hardness of available components**. In principle, many technical solutions are available at different price points.
  - Assuming BaF_2 as the crystal and a generic photosensor + an amplifier/shaper that produces a 30 ns signal, the only real physical limitation (meaning no engineering problem that cannot be solved with money or with future technology) is the pileup.
  - I have heard of a hypothetical factor of 100 increase in the intensity.
    - Assuming that it there is duty factor change x3, the instantaneous luminosity increases by a factor of 33.
    - Assuming a current mean occupancy for the inner ring channels, of 1, each channel would have 33 hits to extract following the muonic atom decay probability function; this would be quite difficult to resolve even with a very fast ADC. So the limitation is the number of 30 ns hits that we can resolve in a microbunch. If we want a stable system, we have to add a factor from 3 to 5 for beam intensity fluctuations.
    - Increasing the calorimeter inner radius can mitigate the problem by a small amount.

Readout techniques

- Ultra Fast ADC (>1 GHz …) – 5x sampling frequency
  - Solves pileup problem
  - High bandwidth, 10 gbit links
  - Expensive
  - High power
  - Needs expensive FPGA. Radiation hardness ?
- TDC
  - Good time resolution
  - PicoTDC under development at CERN
  - Does not necessarily solve pileup issue
- TDC + ADC
  - Can solve pileup problem

- Radiation hardness at a Megarad is challenging
  - PicoTDC ok …
  - FPGA ? Today (2020) only Xilinx Virtex5-QV space grade FPGA are qualified for dose 1 MRad(Si) but $$$$$$$
  - ADC ? Need to be qualified …

Spinella

Mu2e-II calorimeter subgroup

- The only R&D effort that has been communicated to our subgroup over the last year or so is the work at Caltech on doped barium fluoride and on a SiPM for BaF_2 readout
- Neither of these efforts is currently funded
  - COVID-19 restrictions have impacted the work, but there has been some progress
  - We have submitted three proposals seeking funding
    - Rothenberg Innovation Initiative (Caltech) – not funded
    - DOE Advanced Detector Research – excellent reviews, but not funded
    - Caltech/JPL President's and Director's Research and Development Fund – not funded
- We want to organize another calorimeter workshop, but we haven't detected sufficient activity to warrant one
  - Other potential avenues of inquiry include different crystals (*e.g.*, LYSO), nanoparticle wavelength shifters, microchannel PMTs, LAAPDs, …

Photosensor options for BaF_2 readout

- BaF_2 is an excellent candidate for a fast, high rate, radiation-hard crystal for the Mu2e-II calorimeter, provided that one has a way of utilizing the 220 nm fast component without undue interference from the larger 320 nm slow component
    - There are actually two fast components (τ = 0.6 ns) at 195 and 220 nm and two slow components (τ = 630 ns) at 320 and 400 nm

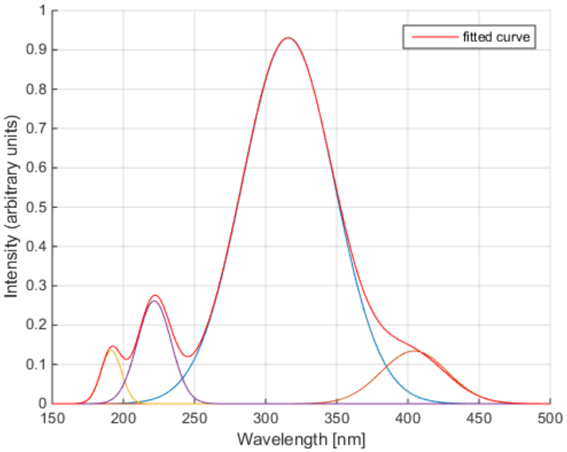

- Our approach

  Suppress the BaF_2 slow component by Y doping, as developed by Zhu *et al.*,: a major advance, although R&D remains to be done

  Develop a SiPM that is sensitive only to the fast component

  This is being done by a Caltech/JPL/FBK collaboration:

Caltech	B. Echenard, D. Hitlin, J. Oyang, J. Trevor, L. Zhang, R-Y. Zhu
JPL	J. Hennessy, M. Hoenk, A. Jewell
FBK	A. Ficorella, A. Gola, G. Paternoster

FBK SiPM with three-layer filter

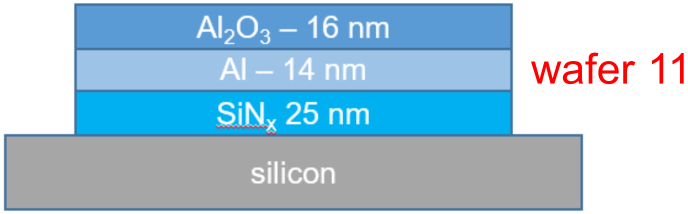

PDE scanned *vs.* wavelength at several bias voltages, with gain measured

Calibrated with pulsed LED @ 465 nm for SiPM bias at 29 V

Excess noise factor determined at each bias

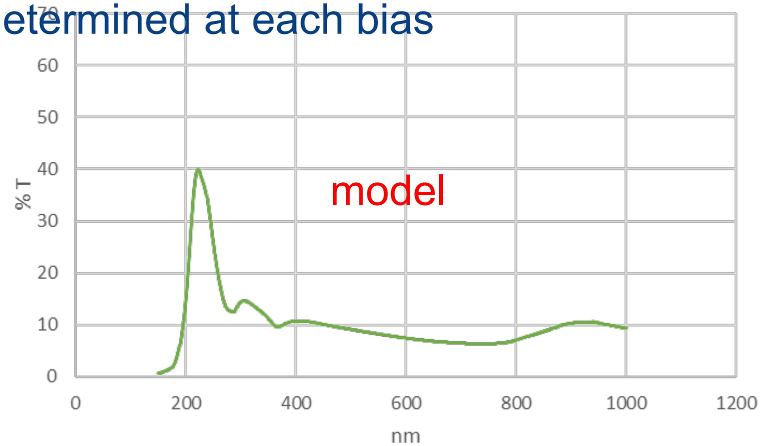

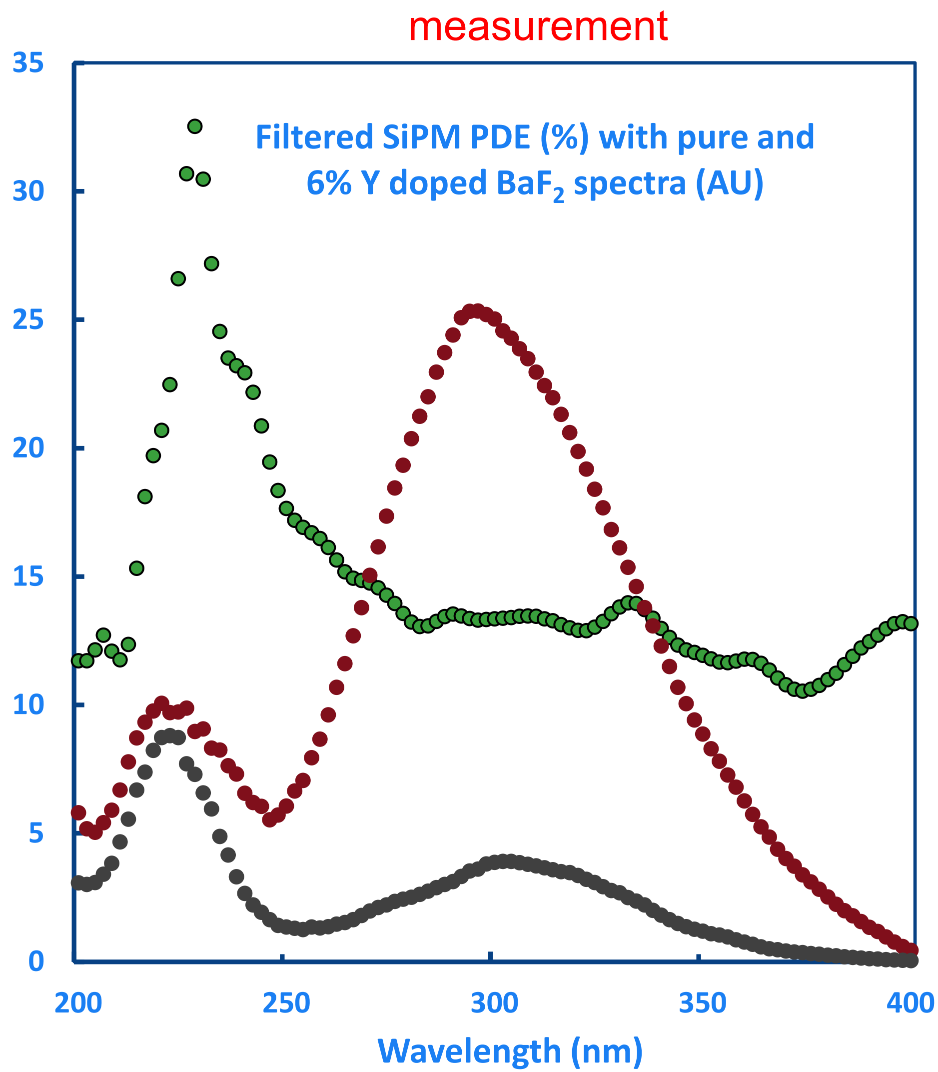

L. Zhang, J. Oyang

FBK #611 BaF_2 Cosmic Ray Spectrum

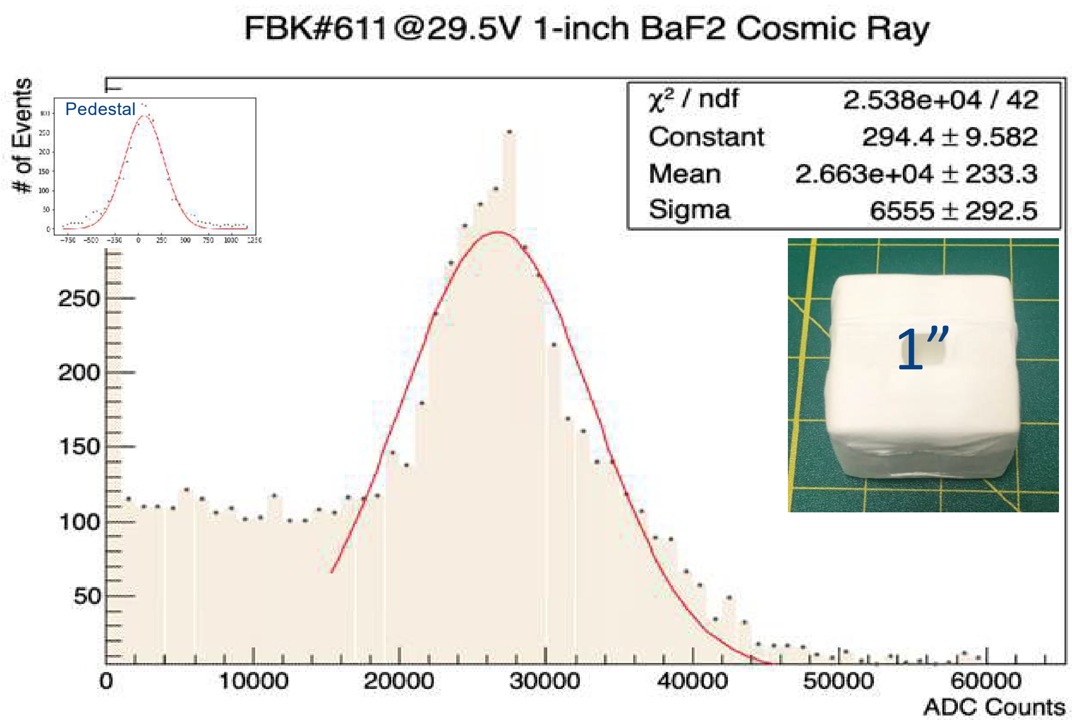

- FBK SiPM #611, dimension 6x6 mm, operated at 29.5V
- BaF_2 dimension 1” x 1” x 1”, wrapped with teflon with an opening of 6x6 (mm)
- Cosmic ray deposits 6.374 MeV/cm * 2.54 cm = 16.2 MeV
- (26631 - 68) adc / 148 pe/adc = 180 pe
- 180 pe / 16.2 MeV = 11 pe/MeV   With 2x3 array, expect 60-70 pe/MeV

Five-layer filter design – calculation

- The bandpass of the five-layer filter (this design assumes complete removal of SiNx passivation) is narrower, encompasses the small 195nm fast component and has superior suppression of the slow component

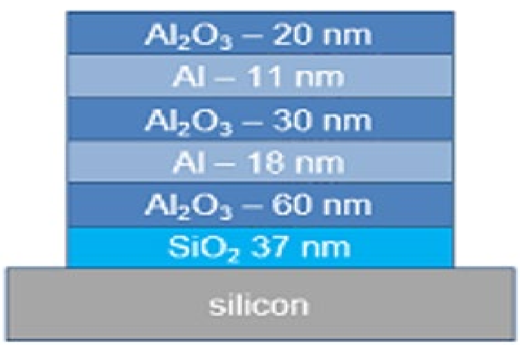

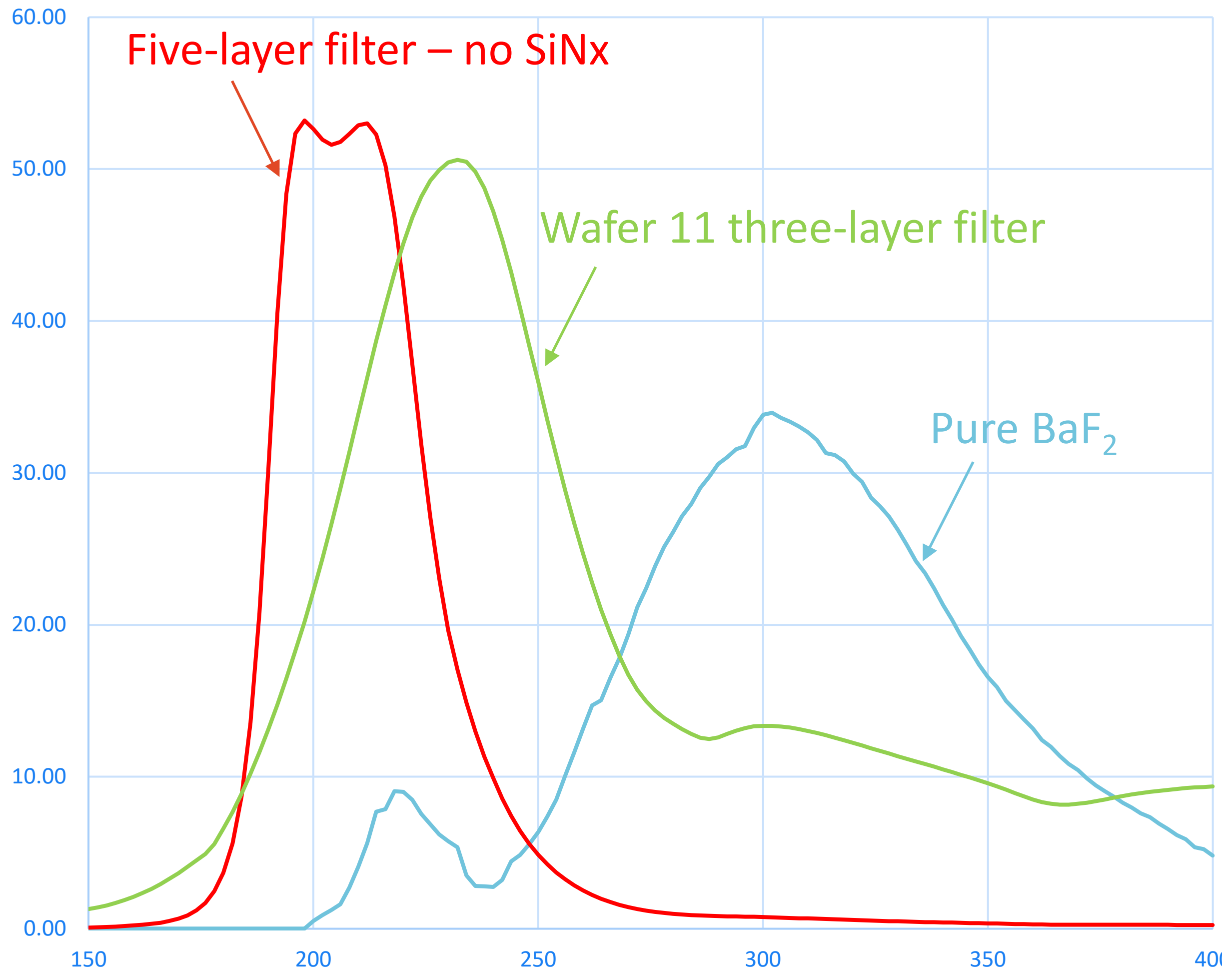

Further improvement of fast/slow performance

- Combining
  - 6% Y-doped BaF_2 and
  - SiPM with a five-layer filter

  provides further improvement in the ratio of fast-to-slow scintillation components
- This performance should be adequate for the Mu2e-II calorimeter and other high-rate applications

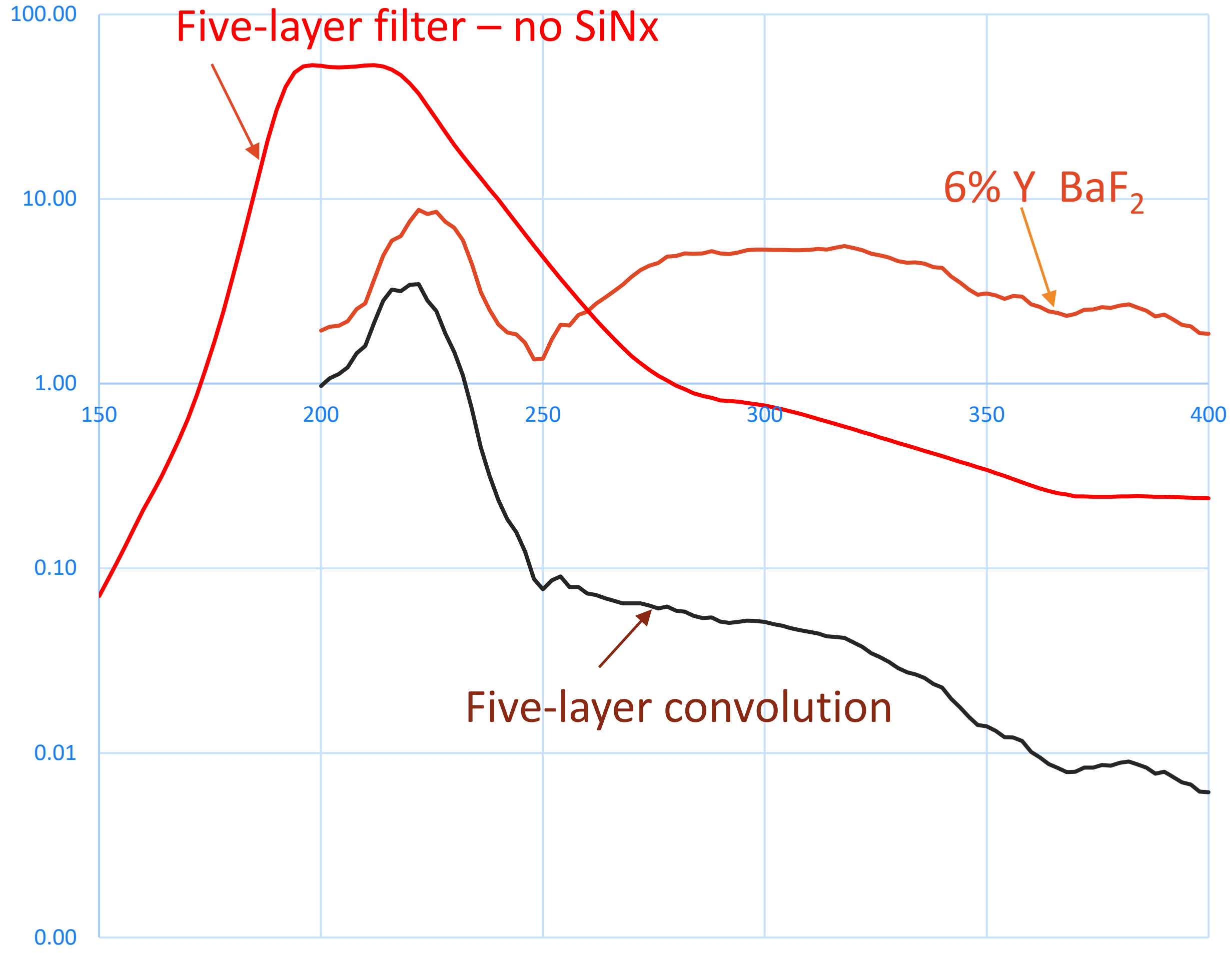

CIT/JPL/FBK SiPM - a phased approach

- Building on our experience with a large area APD developed with RMD, we have adopted a phased SiPM development approach

DONE

1. Build a three layer ALD filter on a 6x6 mm NUV SiPM structure, exploring different SiNx passivation layers, guard ring structures, …
2. Fabricate 2x3 arrays of the 6x6 mm chips, biased in series parallel configuration à la MEG and Mu2e to read out larger crystals

Underway

3. Improve slow component rejection with more sophisticated five-layer filters – devices at Caltech, in queue for measurement/test

Unfunded

4. Use delta doping and backside illumination to improve PDE, the effectiveness of the filter and timing performance
   - First explore parameter space of MBE fab of delta-doping using diode structures of various sizes – reticles have been produced
   - Then fab back-illuminated SiPMs with five-layer filters and delta-doping

Estimated layer thicknesses April 2021

- JPL now has access to their ALD and MBE facilities
- We have now produced new five-layer filters on two existing wafers

- FBK wafers 1 and 18 have pre-existing passivation layers of SiN and SiO_2 respectively
- Dummy wafers B0330 and B0401B were also produced for etch testing, starting with bare silicon only
- These wafers have been sent to FBK for electrical testing, dicing into 6x6 mm chips and production of 3x2 arrays of the 6x6 mm chips
- Devices for measurement of PDE (6x6 mm) were shipped to Caltech yesterday. (3x2 arrays) for readout of large BaF_2 crystals will be shipped in a few weeks

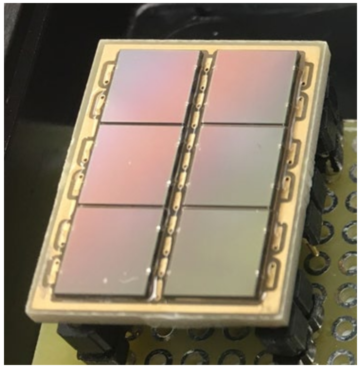

IV curves for new wafers

IV measurement

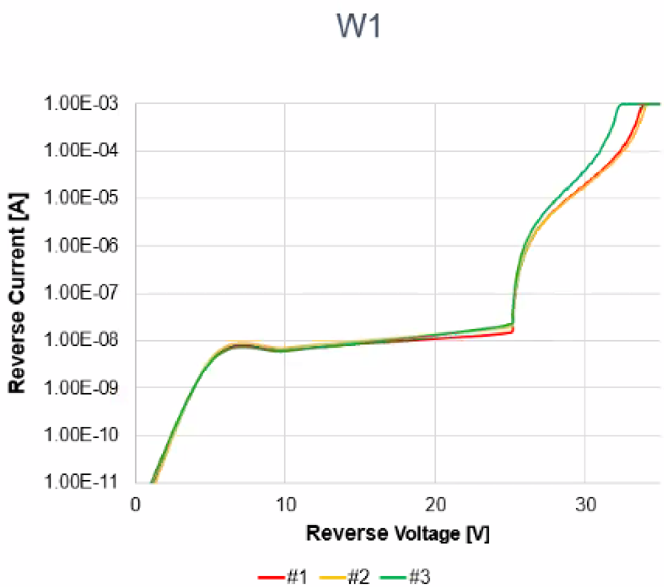

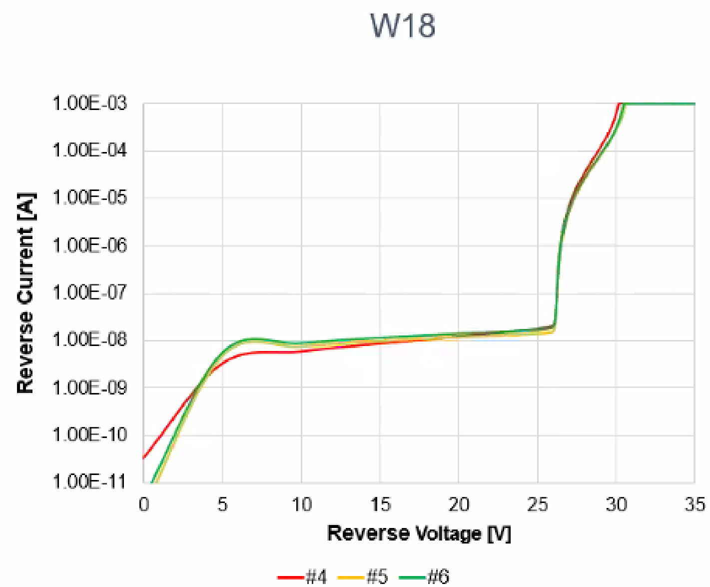

3

Next steps – not currently funded

- We succeeded, using an SBIR grant with RMD several years ago to produce large area back-illuminated APDs with filters for the BaF_2 fast component
- SiPM structures are much more complex
  - We have adopted a two-phase approach
    1. Fabricate diode structures of varying sizes in order to use measurements of leakage current with many area vs. perimeter ratios to understand the effect of
       - Different etching procedures on metallization and other surface structures
       - Different MBE formulations

       on device electrical performance
    1. Use this information to optimize deep, delta-doped and filtered SiPM structures that can be back-illuminated

Photodiode wafers

Shot composition

Splits	Layout	AA/SIR Overlap	Trench/ SIR
1	L1	Overlap1	no Dist
2	L1	Overlap2	no Dist
3	L1	Overlap1	Dist1
4	L1	Overlap2	Dist1
3	L1	Overlap1	Dist2
4	L1	Overlap2	Dist2
5	L2	Overlap1	no Dist
6	L2	Overlap2	no Dist
7	L2	Overlap1	Dist1
8	L2	Overlap2	Dist1
7	L2	Overlap1	Dist2
8	L2	Overlap2	Dist2
9	L3	Overlap1	no Dist
10	L3	Overlap2	no Dist
11	L3	Overlap1	Dist1
12	L3	Overlap2	Dist1
11	L3	Overlap1	Dist2
12	L3	Overlap2	Dist2

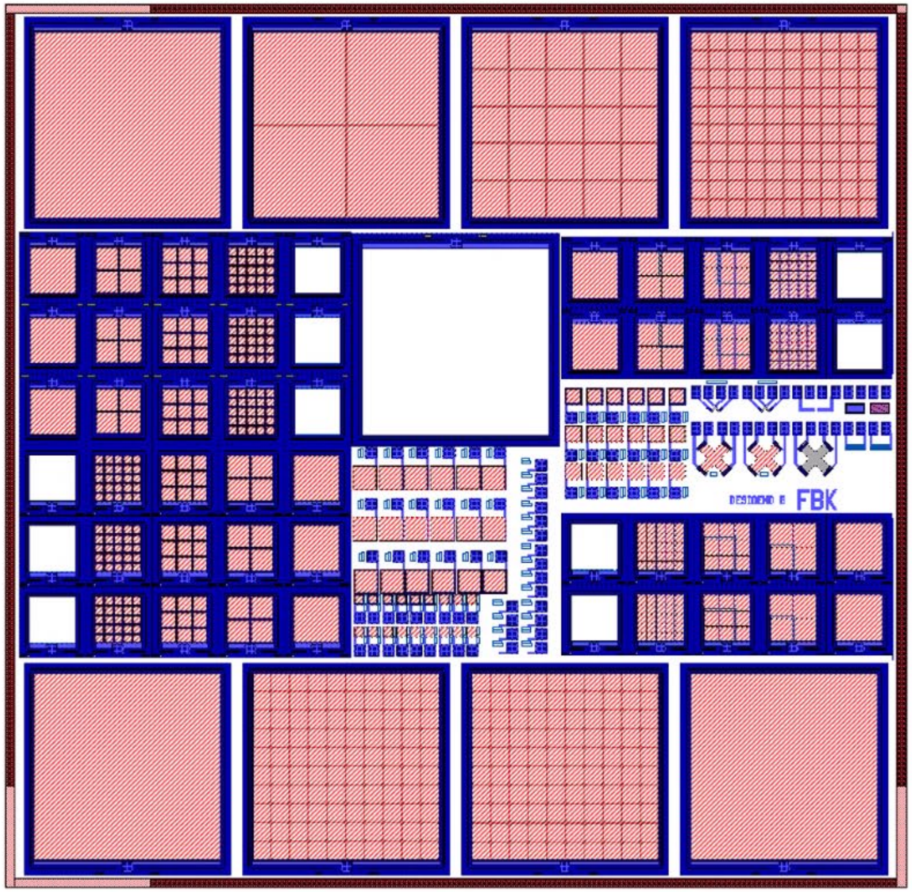

Shot size ~10x10mm^2

2

Photodiode production schedule

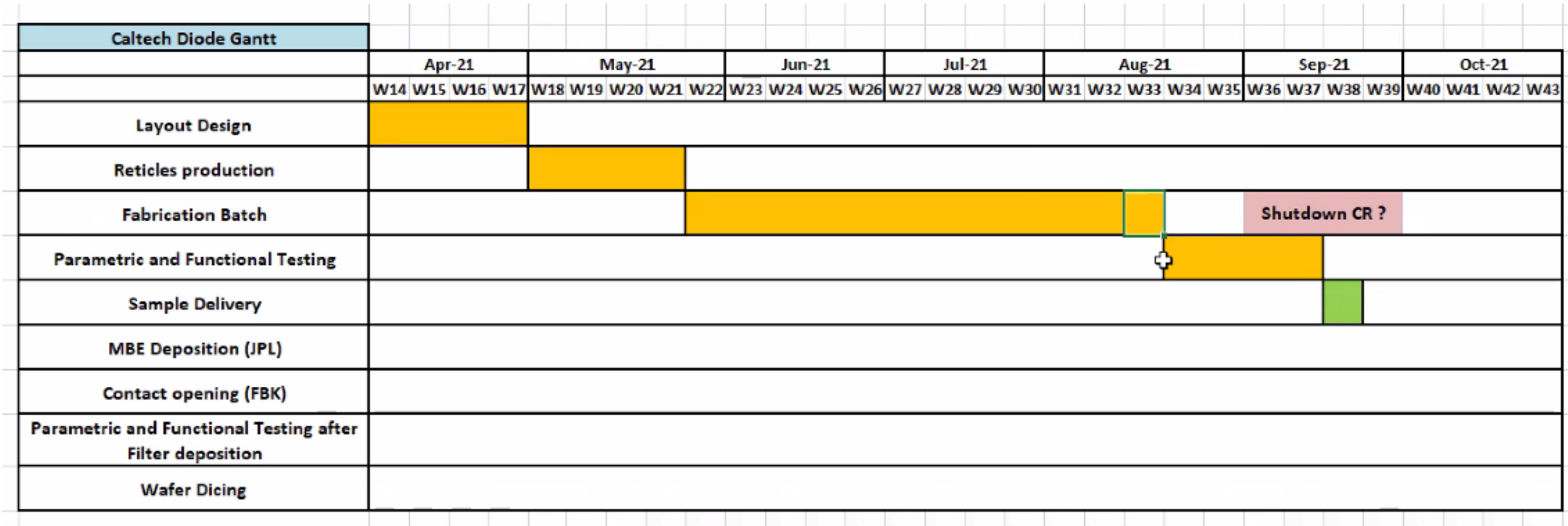

Conclusions

- Further development of crystals (uniformity of Y doping in BaF_2), radiation hardness (ionizing and neutrons) is needed
- Further development of an appropriate photosensor is needed
  - Need neutron irradiation tests
  - Very low temperature performance should be verified
  - Other ramifications of low temperature, such as effect on tracker must be studied
- Partial solutions such as replacing portions of a disk may be viable
- The choice of crystal and photosensor for the Mu2e-II calorimeter will drive the design of the readout system
  - The DAQ system will be challenging
    - Several architectures needs to be carefully evaluated
- We will need both simulations and laboratory prototypes to choose the best solution in terms of performance (bandwidth and radiation hardness) and cost
- Work is ongoing in crystal, sensor and DAQ areas